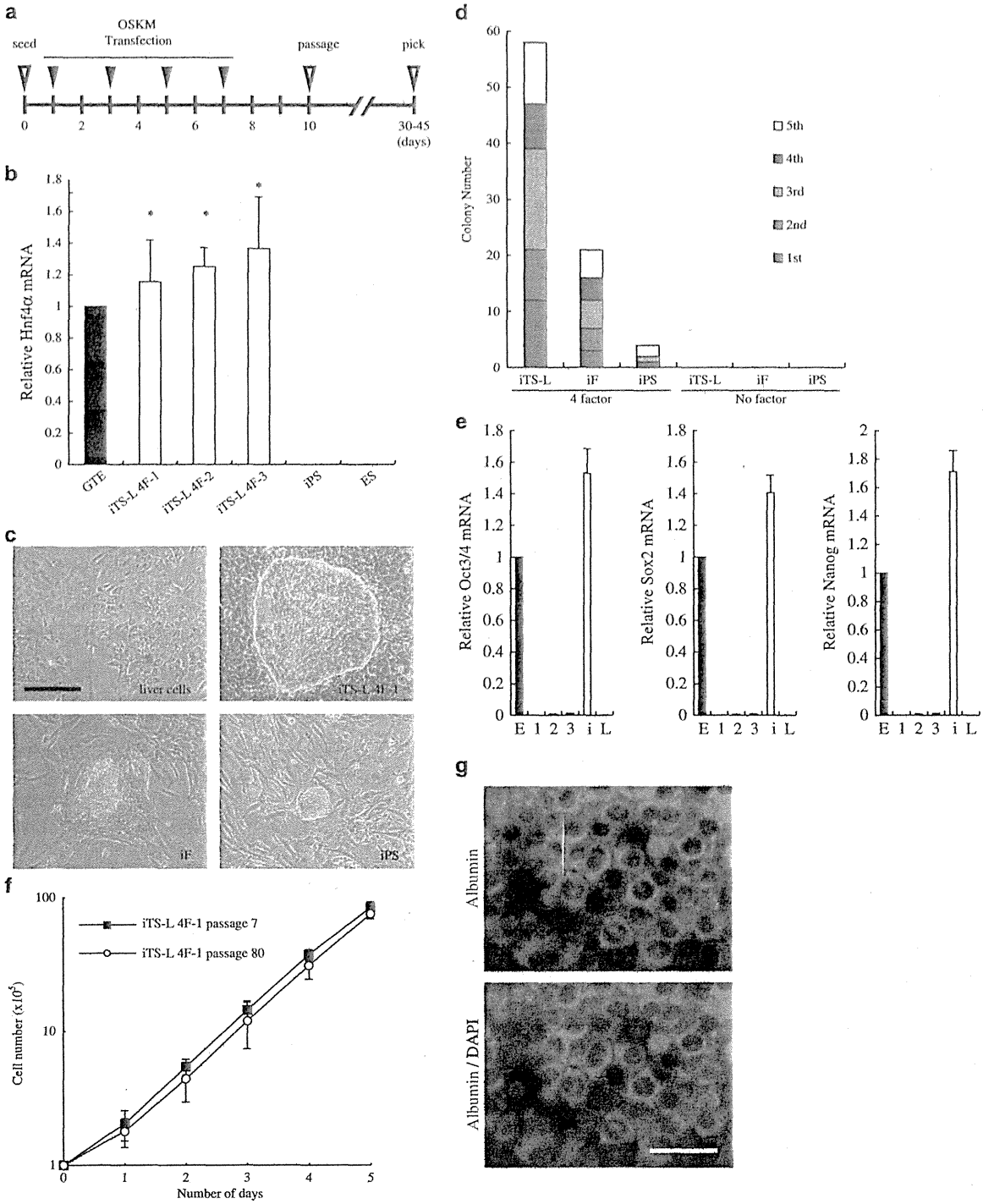

Figure 4 *Generation of iTS-L cells by expression plasmid and Hnf4α selection.* (**a**) The time schedules for the induction of iTS-L cells with the plasmid. Open arrowheads indicate the timing of cell seeding, passaging and colony pickup. Solid arrowheads indicate the timing of transfection. (**b**) Selection of iTS-L cells by a quantitative RT-PCR analysis of the Hnf4α gene in each colony. Each colony was analyzed by quantitative RT-PCR of the Hnf4α gene. The GTE cells derived from ES cells were used as positive control, and iTS-L cells were defined as when the expression level of Hnf4α gene was similar to that in GTE cells. The data are expressed as the Hnf4α gene-to-β-actin ratio, with that of the GTE cells arbitrarily set at 1 ($n=4$). Error bars represent S.E. $^*P<0.05$ compared with iPS cells or ES cells. (**c**) The morphology of the liver cells, iTS-L, iF and iPS cells. Scale bars = 200 μm. (**d**) The colony number of iTS-L cells. The OSKM plasmid was transfected into liver cells from five different mice aged 24 weeks, and the number of colonies was counted after 30–45 days. '1st, 2nd,...' refers to the mouse number. (**e**) The quantitative RT-PCR analysis of the Oct3/4, Sox2 and Nang gene expression in iTS-L 4F cells. ES cells and liver cells (> 95% hepatocyte) were used as controls. The data are expressed as the genes-to-β-actin ratio, with that of the ES cells arbitrarily set at 1 ($n=4$). E, ES cells; 1, iTS-L 4F-1 cells; 2, iTS-L 4F-2 cells; 3, iTS-L 4F-3 cells; i, iPS cells; L, liver cells. Error bars represent S.E. (**f**) Growth curves of iTS-L cells (passage 7 and 80). Error bars represent S.E. (**g**) Immunostaining of albumin-producing cells derived from iTS-L 4F-1 cells. Scale bars = 50 μm

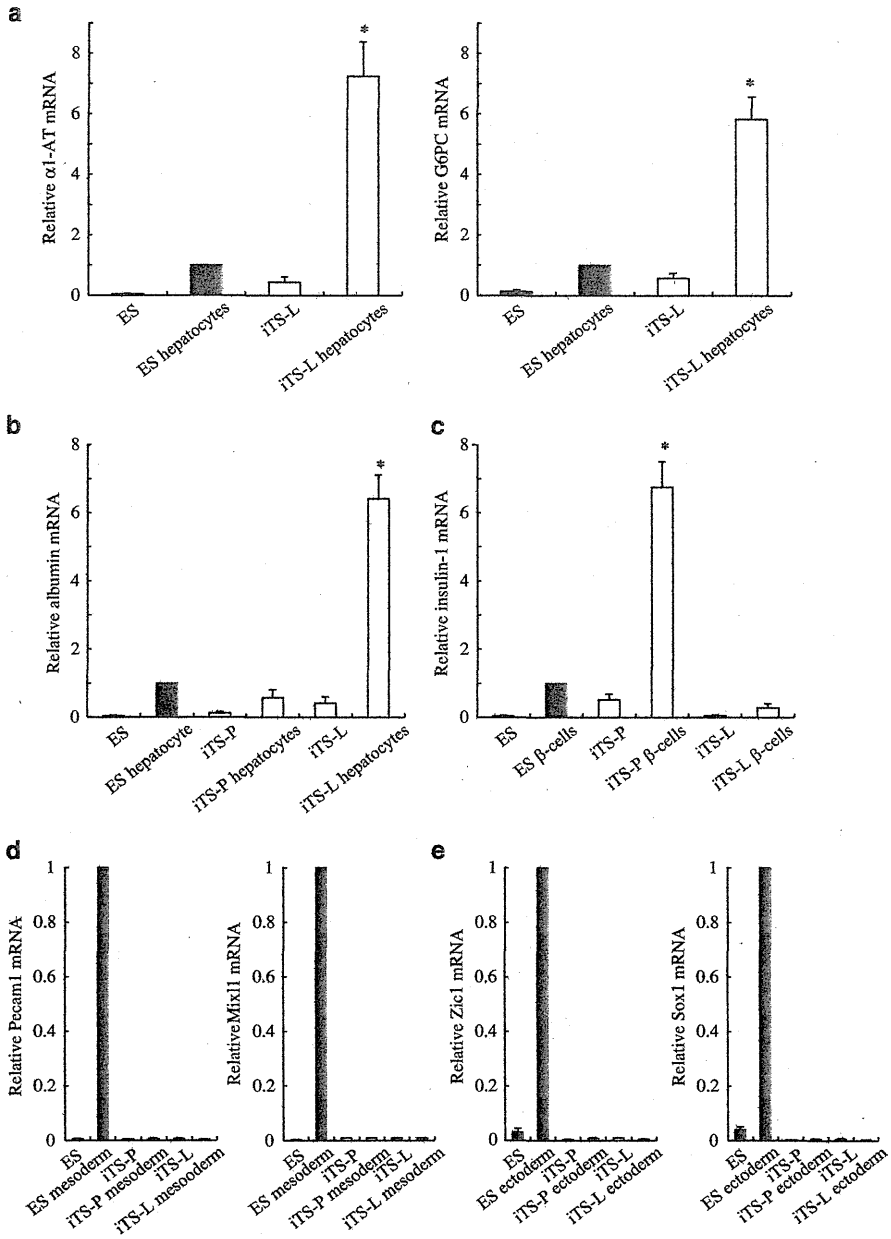

Figure 5 Differentiation of iTS-L cells into hepatocytes and restriction of iTS cell developmental potential. (**a**) The quantitative RT-PCR analysis of the α1-AT and G6PC genes in differentiated iTS-L cells. Differentiated cells derived from iTS-L 4F-1 cells (passage 45) were analyzed by quantitative RT-PCR. *$P<0.05$ compared with iTS-L cells or ES cells. (**b**) The quantitative RT-PCR analysis of the albumin gene in differentiated or undifferentiated iTS-P/iTS-L cells. *$P<0.05$ compared with other cells. (**c**) The quantitative RT-PCR analysis of the insulin-1 gene in differentiated or undifferentiated iTS-P/iTS-L cells. *$P<0.05$ compared with other cells. (**d**) The quantitative RT-PCR analysis of mesodermal genes (Pecam1 and Mixl1) in differentiated or undifferentiated iTS-P/iTS-L cells. (**e**) The quantitative RT-PCR analysis of neuroectodermal genes (Zic1 and Sox1) in differentiated or undifferentiated iTS-P/iTS-L cells. iTS-P 4F-1 and iTS-L 4F-1 cells and the differentiated cells derived from iTS-P 4F-1 and iTS-L 4F-1 cells (passage 45) were analyzed by quantitative RT-PCR. ES cells and the differentiated cells derived from ES cells were used as controls. The data are expressed as the genes-to-β-actin ratio, with that of the differentiated cells from ES cells arbitrarily set at 1 ($n=4$). Error bars represent S.E.

pancreas/liver cells and that acquire self-renewal potential. Cheng *et al.* recently reported self-renewing endodermal progenitor (EP) cell lines derived from human ES/iPS cells. Their EP cells differentiated into numerous endodermal lineages, including pancreatic β cells, hepatocytes and intestinal epithelia, but not ectodermal/mesodermal lineages. Moreover, the EP cells were non-tumorigenic *in vivo*.[23] These findings also support the generation of iTS-P/iTS-L cells, which are non-tumorigenic *in vivo*.

Some groups have shown that overexpression of Pdx1, Ngn3, NeuroD and/or MafA by adenoviruses *in vivo* directly converted liver cells[32–34] or pancreatic tissue[35] into IPC, suggesting that direct reprogramming without reversion to a pluripotent stem cell state is possible. These reports of direct

reprogramming without reversion to a pluripotent stem cell state seem to have fewer related ethical issues than iPS cells. However, these strategies require a large number of mature cells, and the induction therapy has to be done on all of these cells directly, because they are not stem cells and do not have self-renewal capacity. Two major advantages of iPS/iTS cells are that they can be generated from a small number of cells, and they will expand to a sufficient number of cells because they have self-renewal capacity.

In this study, we used crude material instead of defined pancreatic populations. Our recent study showed that iTS-P cells can be generated from both islet and non-islet cell populations. Moreover, we recently established iTS-P cells using the pancreatic tissue of NOD mice, suggesting that iTS-P cells can be generated from pancreatic cells derived from patients with type 1 diabetes.

In conclusion, we generated iTS cells from mouse pancreas/liver cells by transient overexpression of reprogramming factors and tissue-specific selection. The generation of iTS-P/iTS-L cells and their differentiation into IPC/hepatocytes have important implications due to their potential use for autologous cell replacement therapy, and because they appear to be more easily and efficiently differentiated than ES cells. The technology to generate iTS cells by reprogramming factors and tissue-specific selection may also be useful for the generation of other tissue-specific stem cells.

Materials and Methods

Mice and cell culture. All mouse studies were approved by the review committee of Okayama University Graduate School of Medicine, Dentistry and Pharmaceutical Sciences and Chiba-East National Hospital, National Hospital Organization. The 24-week-old C57/BL6 mice (CREA) were used for primary pancreatic/liver tissue preparations. Each mouse pancreas/liver was digested with 2 ml cold M199 medium containing 2 mg/ml collagenase (Roche Diagnostics Corporation, Indianapolis, IN, USA). The digested tissues were cultured in Dulbecco's modified Eagle's medium (DMEM; Life Technologies, Carlsbad, CA, USA) with 10–20% fetal bovine serum (FBS; BIO-WEST, Inc., Logan, UT, USA). The 8-week-old nude or NOD/scid mice (CREA) were used for teratoma formation studies.

Mouse ES cells (ATCC, Manassas, VA, USA), iPS cells and iTS cells were maintained in complete ES cell media w/15% FBS (Millipore, Billerica, MA, USA) on feeder layers of mitomycin C-treated STO or SNB cells, as described previously.[1,36] ES cells were passaged every 3 days, and iTS cells were passaged every 5 days.

Plasmid construction and transfection. To generate the OSKM plasmid, the cDNAs encoding Oct3/4, Sox2, Klf4 and c-Myc were connected in this order with the 2A peptide and inserted into a plasmid containing the CMV promoter. The OKS (Addgene, Cambridge, MA, USA: Plasmid 19771 (pCX-OKS-2A)) or OSKM plasmid was transfected into pancreas/liver cells from 24-week-old mice on days 1, 3, 5 and 7, as previously described.[8] Colonies were manually picked at 30–45 days after first transfection. To attempt efficient selection of iTS-P cells, we used a plasmid containing a NeoR gene that was driven by the Pdx1 promoter (pPdx1). To generate the pPdx1-NeoR plasmid, the Cre gene in the Pdx1-Cre plasmid (Addgene: Plasmid 15021 (DM#258); https://www.addgene.org/15021/) was replaced with the NeoR gene, derived from pIRES-neo (Clontech, Mountain View, CA, USA). The detail protocol is shown in Supplementary Information.

DNA purification and PCR. DNA was extracted from cells using the AllPrep DNA/RNA Mini Kit (Qiagen, Tokyo, Japan). Polymerization reactions were performed in a Perkin-Elmer 9700 Thermocycler with 3 μl cDNA (20 ng DNA equivalents), 160 μmol/l cold dNTPs, 10 pmol appropriate oligonucleotide primers, 1.5 mmol/l $MgCl_2$ and 5 U AmpliTaq Gold DNA polymerase (Perkin-Elmer, Norwalk, CT, USA) in 1 × PCR buffer. The oligonucleotide primers are shown in Supplementary Table 1. The thermal cycle profile used a 10-min denaturing step at 94 °C, followed by amplification cycles (1 min denaturation at 94 °C, 1 min annealing at 57–62 °C and 1 min extension at 72 °C) with a final extension step of 10 min at 72 °C.

RT-PCR/quantitative PCR. Total RNA was extracted from cells using the AllPrep DNA/RNA Mini Kit or RNeasy Mini Kit (Qiagen). After quantifying the RNA by spectrophotometry, 2.5 μg of RNA was heated at 85 °C for 3 min and then reverse transcribed into cDNA in a 25-μl solution containing 200 U of Superscript II RNase H-RT (Life Technologies), 50 ng random hexamers (Life Technologies), 160 μmol/l dNTP and 10 nmol/l dithiothreitol. The reaction consisted of 10 min at 25 °C, 60 min at 42 °C and 10 min at 95 °C. Polymerization reactions were performed as shown in the DNA purification and PCR section. The oligonucleotide primers are shown in Supplementary Table 1.

Quantification of the mRNA levels was carried out using the TaqMan real-time PCR system, according to the manufacturer's instructions (Applied Biosystems, Foster City, CA, USA). PCR was performed for 40 cycles, including 2 min at 50 °C and 10 min at 95 °C as initial steps. In each cycle, denaturation was performed for 15 s at 95 °C and annealing/extension was performed for 1 min at 60 °C. PCR was carried out in 20 μl of solution using cDNAs synthesized from 1.11 ng of total RNA. For each sample, the expression of mRNA was normalized by dividing the β-actin expression level. Primers for mouse insulin-1, insulin-2, α1-AT, G6PC, albumin, Pecam1, Mixl1, Zic1, Sox1, Oct3/4, Sox2, Nanog, Sox17, Hnf4α, Pdx1 and β-actin are commercially available (Assays-on-Demand Gene Expression Products; Applied Biosystems).

Cell induction and differentiation. Directed differentiation into IPC was conducted as described previously,[21,22] with minor modifications. ES cells, iPS cells (passage 45), iTS-P cells (passage 45 and 80) were used in this experiment. In stage 1, cells were treated with 25 ng/ml of Wnt3a and 100 ng/ml of activin A (R&D Systems, Minneapolis, MN, USA) in RPMI (Life Technologies) for 1 day, followed by treatment with 100 ng/ml of activin A in RPMI + 0.2% FBS for 2 days. In stage 2, the cells were treated with 50 ng/ml of FGF10 (R&D Systems) and 0.25 μM of KAAD-cyclopamine (Toronto Research Chemicals, Toronto, ON, Canada) in RPMI + 2% FBS for 3 days. In stage 3, the cells were treated with 50 ng/ml of FGF10, 0.25 μM of KAAD-cyclopamine and 2 μM of all-*trans* retinoic acid (Sigma-Aldrich, St. Louis, MO, USA) in DMEM + 1% (vol/vol) B27 supplement (Life Technologies) for 3 days. In stage 4, the cells were treated with 1 μM of DAPT (Sigma-Aldrich) and 50 ng/ml of exendin-4 (Sigma-Aldrich) in DMEM + 1% (vol/vol) B27 supplement for 3 days. In stage 5, the cells were then treated with 50 ng/ml of exendin-4, 50 ng/ml of IGF-1 (Sigma-Aldrich) and 50 ng/ml of HGF (R&D Systems) in CMRL (Life Technologies) + 1% (vol/vol) B27 supplement for 3–6 days. Differentiation into hepatocytes, neuroectoderm or mesoderm was conducted as reported previously.[23,24]

Teratoma formation/tumorigenicity assay. A total of 1×10^6–1×10^7 of iPS/iTS cells were inoculated into one thigh each of nude or NOD/scid mice. As a positive control, we transplanted 1×10^6 ES cells or iPS cells into the other thigh of the nude or NOD/scid mice.

Immunostaining. Cells were fixed with 4% paraformaldehyde in PBS buffer. After blocking with 20% AquaBlock (EastCoast Bio, North Berwick, ME, USA) for 30 min at room temperature, the cells were incubated overnight at 4 °C with a goat anti-insulin antibody (1 : 100; Abcam, Tokyo, Japan), rabbit anti-C-peptide antibody (1 : 100; Cell Signaling Technology, Danvers, MA, USA), rabbit anti-Pdx1 antiserum[37] (1 : 1000) or rabbit anti-albumin (Cedarline, Gymea, NSW, Australia) and then for 1 h at room temperature with FITC-conjugated anti-goat IgG (1 : 250; Abcam), Alexa Fluor 647-conjugated anti-rabbit IgG (1 : 250; Cell Signaling Technology) or FITC-conjugated anti-rabbit IgG (1 : 100; Jackson Immunochemicals, West Grove, PA, USA). Mounting medium for fluorescence with DAPI (Vector Laboratories, Peterborough, UK) was used for mounting. Percentage of insulin/C-peptide-positive cells was calculated by ratio of immunostaining positive cells/DAPI-positive cells in 10 visual fields.

Insulin release assay. The insulin release was measured by incubating the cells in Functionality/Viability Medium CMRL1066 (Mediatech, Inc., Manassas, VA, USA). The cells were washed three times in PBS and incubated in the solution (Functionality/Viability Medium CMRL1066) with 2.8 mM D-glucose six times for 20 min (total 2 h) each to wash them. The cells were then incubated in the solution with 2.8 mM D-glucose for 2 h, and then in the solution with 20 mM D-glucose for

2 h. The insulin levels in the culture supernatants were measured using an Ultra Sensitive Mouse Insulin ELISA (enzyme-linked immunosorbent assay) kit (Mercodia, Uppsala, Sweden). The stimulation index was calculated by dividing the insulin values measured from the 20 mM glucose samples by 2.8 mM glucose samples.

Statistical analyses. The data are expressed as the means ± S.E. Two groups were compared using Student's *t*-test. The differences between each group were considered to be significant if the *P*-value was <0.05.

Conflict of Interest

The authors declare no conflict of interest.

Acknowledgements. This work was supported in part by the Japan Society for the Promotion of Science and the Ministry of Health, Labour and Welfare.

Author contributions

HN designed the experiments and analyzed the data. HN carried out most of the experimental work with the help of IS and TT. HK, MW and YN provided materials and discussion. HN wrote the manuscript. All authors discussed and commented on the manuscript.

1. Takahashi K, Yamanaka S. Induction of pluripotent stem cells from mouse embryonic and adult fibroblast cultures by defined factors. *Cell* 2006; **126**: 663–676.
2. Takahashi K, Tanabe K, Ohnuki M, Narita M, Ichisaka T, Tomoda K *et al.* Induction of pluripotent stem cells from adult human fibroblasts by defined factors. *Cell* 2007; **131**: 861–872.
3. Yu J, Vodyanik MA, Smuga-Otto K, Antosiewicz-Bourget J, Frane JL, Tian S *et al.* Induced pluripotent stem cell lines derived from human somatic cells. *Science* 2007; **318**: 1917–1920.
4. Park IH, Zhao R, West JA, Yabuuchi A, Huo H, Ince TA *et al.* Reprogramming of human somatic cells to pluripotency with defined factors. *Nature* 2008; **451**: 141–146.
5. Maherali N, Sridharan R, Xie W, Utikal J, Eminli S, Arnold K *et al.* Directly reprogrammed fibroblasts show global epigenetic remodeling and widespread tissue contribution. *Cell Stem Cell* 2007; **1**: 55–70.
6. Okita K, Ichisaka T, Yamanaka S. Generation of germline-competent induced pluripotent stem cells. *Nature* 2007; **448**: 313–317.
7. Wernig M, Meissner A, Foreman R, Brambrink T, Ku M, Hochedlinger K *et al.* In vitro reprogramming of fibroblasts into a pluripotent ES-cell-like state. *Nature* 2007; **448**: 318–324.
8. Okita K, Nakagawa M, Hyenjong H, Ichisaka T, Yamanaka S. Generation of mouse induced pluripotent stem cells without viral vectors. *Science* 2008; **322**: 949–953.
9. Stadtfeld M, Nagaya M, Utikal J, Weir G, Hochedlinger K. Induced pluripotent stem cells generated without viral integration. *Science* 2008; **322**: 945–949.
10. Yu J, Hu K, Smuga-Otto K, Tian S, Stewart R, Slukvin II *et al.* Human induced pluripotent stem cells free of vector and transgene sequences. *Science* 2009; **324**: 797–801.
11. Okita K, Matsumura Y, Sato Y, Okada A, Morizane A, Okamoto S *et al.* A more efficient method to generate integration-free human iPS cells. *Nat Methods* 2011; **8**: 409–412.
12. Bonner-Weir S, Taneja M, Weir GC, Tatarkiewicz K, Song KH, Sharma A *et al.* In vitro cultivation of human islets from expanded ductal tissue. *Proc Natl Acad Sci USA* 2000; **97**: 7999–8004.
13. Heremans Y, Van De Casteele M, in't Veld P, Gradwohl G, Serup P, Madsen O *et al.* Recapitulation of embryonic neuroendocrine differentiation in adult human pancreatic duct cells expressing neurogenin 3. *J Cell Biol* 2002; **159**: 303–312.
14. Gao R, Ustinov J, Pulkkinen MA, Lundin K, Korsgren O, Otonkoski T. Characterization of endocrine progenitor cells and critical factors for their differentiation in human adult pancreatic cell culture. *Diabetes* 2003; **52**: 2007–2015.
15. Street CN, Lakey JR, Shapiro AM, Imes S, Rajotte RV, Ryan EA *et al.* Islet graft assessment in the Edmonton Protocol: implications for predicting long-term clinical outcome. *Diabetes* 2004; **53**: 3107–3114.
16. Yamamoto T, Yamato E, Taniguchi H, Shimoda M, Tashiro F, Hosoi M *et al.* Stimulation of cAMP signalling allows isolation of clonal pancreatic precursor cells from adult mouse pancreas. *Diabetologia* 2006; **49**: 2359–2367.
17. Noguchi H, Oishi K, Ueda M, Yukawa H, Hayashi S, Kobayashi N *et al.* Establishment of mouse pancreatic stem cell line. *Cell Transplant* 2009; **18**: 563–571.
18. Kuise T, Noguchi H, Saitoh I, Kataoka HU, Watanabe M, Fujiwara T. Isolation efficiency of mouse pancreatic stem cells is age-dependent. *Cell Med* 2013; **5**: 69–73.
19. Noguchi H, Naziruddin B, Jackson A, Shimoda M, Ikemoto T, Fujita Y *et al.* Characterization of human pancreatic progenitor cells. *Cell Transplant* 2010; **19**: 879–886.
20. Niwa H, Yamamura K, Miyazaki J.. Efficient selection for high-expression transfectants with a novel eukaryotic vector. *Gene* 1991; **108**: 193–199.
21. D'Amour KA, Bang AG, Eliazer S, Kelly OG, Agulnick AD, Smart NG *et al.* Production of pancreatic hormone-expressing endocrine cells from human embryonic stem cells. *Nat Biotechnol* 2006; **24**: 1392–1401.
22. Kroon E, Martinson LA, Kadoya K, Bang AG, Kelly OG, Eliazer S *et al.* Pancreatic endoderm derived from human embryonic stem cells generates glucose-responsive insulin-secreting cells in vivo. *Nat Biotechnol* 2008; **26**: 443–452.
23. Cheng X, Ying L, Lu L, Galvão AM, Mills JA, Lin HC *et al.* Self-renewing endodermal progenitor lines generated from human pluripotent stem cells. *Cell Stem Cell* 2012; **10**: 371–384.
24. Greber B, Coulon P, Zhang M, Moritz S, Frank S, Müller-Molina AJ *et al.* FGF signalling inhibits neural induction in human embryonic stem cells. *EMBO J* 2011; **30**: 4874–4884.
25. Shapiro AM, Lakey JR, Ryan EA, Korbutt GS, Toth E, Warnock GL *et al.* Islet transplantation in seven patients with type 1 diabetes mellitus using a glucocorticoid-free immunosuppressive regimen. *N Engl J Med* 2000; **343**: 230–238.
26. Kim K, Doi A, Wen B, Ng K, Zhao R, Cahan P *et al.* Epigenetic memory in induced pluripotent stem cells. *Nature* 2010; **467**: 285–290.
27. Polo JM, Liu S, Figueroa ME, Kulalert W, Eminli S, Tan KY *et al.* Cell type of origin influences the molecular and functional properties of mouse induced pluripotent stem cells. *Nat Biotechnol* 2010; **28**: 848–855.
28. Doi A, Park IH, Wen B, Murakami P, Aryee MJ, Irizarry R *et al.* Differential methylation of tissue- and cancer-specific CpG island shores distinguishes human induced pluripotent stem cells, embryonic stem cells and fibroblasts. *Nat Genet* 2009; **41**: 1350–1353.
29. Lister R, Pelizzola M, Kida YS, Hawkins RD, Nery JR, Hon G *et al.* Hotspots of aberrant epigenomic reprogramming in human induced pluripotent stem cells. *Nature* 2011; **471**: 68–73.
30. Ohi Y, Qin H, Hong C, Blouin L, Polo JM, Guo T *et al.* Incomplete DNA methylation underlies a transcriptional memory of somatic cells in human iPS cells. *Nat Cell Biol* 2011; **13**: 541–549.
31. Bar-Nur O, Russ HA, Efrat S, Benvenisty N. Epigenetic memory and preferential lineage-specific differentiation in induced pluripotent stem cells derived from human pancreatic islet beta cells. *Cell Stem Cell* 2011; **9**: 17–23.
32. Ferber S, Halkin A, Cohen H, Ber I, Einav Y, Goldberg I *et al.* Pancreatic and duodenal homeobox gene 1 induces expression of insulin genes in liver and ameliorates streptozotocin-induced hyperglycemia. *Nat Med* 2000; **6**: 568–572.
33. Kaneto H, Matsuoka TA, Nakatani Y, Miyatsuka T, Matsuhisa M, Hori M *et al.* A crucial role of MafA as a novel therapeutic target for diabetes. *J Biol Chem* 2005; **280**: 15047–15052.
34. Kaneto H, Nakatani Y, Miyatsuka T, Matsuoka TA, Matsuhisa M, Hori M *et al.* PDX-1/VP16 fusion protein, together with NeuroD or Ngn3, markedly induces insulin gene transcription and ameliorates glucose tolerance. *Diabetes* 2005; **54**: 1009–1022.
35. Zhou Q, Brown J, Kanarek A, Rajagopa,l J, Melton DA. *In vivo* reprogramming of adult pancreatic exocrine cells to beta-cells. *Nature* 2008; **455**: 627–632.
36. Saitoh I, Sato M, Iwase Y, Inada E, Nomura T, Akasaka E *et al.* Generation of mouse STO feeder cell lines that confer resistance to several types of selective drugs. *Cell Med* 2012; **3**: 97–102.
37. Noguchi H, Kaneto H, Weir GC, Bonner-Weir S. PDX-1 protein containing its own antennapedia-like protein transduction domain can transduce pancreatic duct and islet cells. *Diabetes* 2003; **52**: 1732–1737.

Supplementary Information accompanies this paper on Cell Death and Differentiation website (http://www.nature.com/cdd)

OPEN ACCESS Freely available online

PLOS | ONE

Novel Positively Charged Nanoparticle Labeling for *In Vivo* Imaging of Adipose Tissue-Derived Stem Cells

Hiroshi Yukawa[1]*, Shingo Nakagawa[2], Yasuma Yoshizumi[2], Masaki Watanabe[3], Hiroaki Saito[4], Yoshitaka Miyamoto[5], Hirofumi Noguchi[6], Koichi Oishi[7], Kenji Ono[7], Makoto Sawada[7], Ichiro Kato[4], Daisuke Onoshima[8], Momoko Obayashi[1], Yumi Hayashi[2], Noritada Kaji[1,3], Tetsuya Ishikawa[2], Shuji Hayashi[5], Yoshinobu Baba[1,3,9]

1 Research Center for Innovative Nanobiodevices, Nagoya University, Furo-cho, Chikusa-ku, Nagoya 464-8603, Japan, **2** Department of Medical Technology, Nagoya University, Graduate School of Medicine, Daikominami, Higashi-ku, Nagoya 461-8673, Japan, **3** Department of Applied Chemistry, Graduate School of Engineering, Nagoya University, Furo-cho, Chikusa-ku, Nagoya 464-8603, Japan, **4** Nagoya Research Laboratory, MEITO Sangyo Co., Ltd., Kiyosu 452-0067, Japan, **5** Department of Advanced Medicine in Biotechnology and Robotics, Graduate School of Medicine, Nagoya University, Higashi-ku, Nagoya 461-0047, Japan, **6** Department of Regenerative Medicine, Graduate School of Medicine, University of the Ryukyus, 207 Uehara, Nishihara, Okinawa 903-0215, Japan, **7** Research Institute of Environmental Medicine, Stress Adaption and Protection, Nagoya University, Furo-cho, Chikusa-ku, Nagoya, 464-8601, Japan, **8** Institute of Innovative for Future Society, Nagoya University, Furo-cho, Chikusa-ku, Nagoya 464-8603, Japan, **9** Health Research Institute, National Institute of Advanced Industrial Science and Technology (AIST), Hayashi-cho 2217-14, Takamatsu 761-0395, Japan

Abstract

Stem cell transplantation has been expected to have various applications for regenerative medicine. However, in order to detect and trace the transplanted stem cells in the body, non-invasive and widely clinically available cell imaging technologies are required. In this paper, we focused on magnetic resonance (MR) imaging technology, and investigated whether the trimethylamino dextran-coated magnetic iron oxide nanoparticle -03 (TMADM-03), which was newly developed by our group, could be used for labeling adipose tissue-derived stem cells (ASCs) as a contrast agent. No cytotoxicity was observed in ASCs transduced with less than 100 μg-Fe/mL of TMADM-03 after a one hour transduction time. The transduction efficiency of TMADM-03 into ASCs was about four-fold more efficient than that of the alkali-treated dextran-coated magnetic iron oxide nanoparticle (ATDM), which is a major component of commercially available contrast agents such as ferucarbotran (Resovist), and the level of labeling was maintained for at least two weeks. In addition, the differentiation ability of ASCs labeled with TMADM-03 and their ability to produce cytokines such as hepatocyte growth factor (HGF), vascular endothelial growth factor (VEGF) and prostaglandin E2 (PGE2), were confirmed to be maintained. The ASCs labeled with TMADM-03 were transplanted into the left kidney capsule of a mouse. The labeled ASCs could be imaged with good contrast using a 1T MR imaging system. These data suggest that TMADM-03 can therefore be utilized as a contrast agent for the MR imaging of stem cells.

Citation: Yukawa H, Nakagawa S, Yoshizumi Y, Watanabe M, Saito H, et al. (2014) Novel Positively Charged Nanoparticle Labeling for *In Vivo* Imaging of Adipose Tissue-Derived Stem Cells. PLoS ONE 9(11): e110142. doi:10.1371/journal.pone.0110142

Editor: Xing-Ming Shi, Georgia Regents University, United States of America

Received January 17, 2014; **Accepted** September 16, 2014; **Published** November 3, 2014

Funding: This research was supported by the Cabinet Office, Government of Japan and the Japan Society for the Promotion of Science (JSPS) through the Funding Program for World- Leading Innovative R& D on Science and Technology (FIRST Program) and partially supported by the Japan Science and Technology Agency (JST) through its "Research Center Network for Realization of Regenerative Medicine. The funders had no role in study design, data collection and analysis, decision to publish, or preparation of the manuscript.

Competing Interests: The authors have read the journal's policy and have the following conflicts: Hiroaki Saito and Ichiro Kato have ownership of stocks and paid employment at Meito Sangyo, Inc. The following authors have no competing interests: Hiroshi Yukawa, Watanabe Masaki, Yoshitaka Miyamoto, Noritada Kaji, Hirofumi Noguchi, Koichi Oishi, Kenji Ono, Makoto Sawada, Daisuke Onoshima, Yumi Hayashi, Tetsuya Ishikawa, Shuji Hayashi, Yoshinobu Baba. MEITO Sangyo Co., Ltd. provided the nanoparticles used in this study (Trimethylamino dextran-coated, magnetic iron oxide nanoparticles (TMADM-03)). This does not alter the authors' adherence to all the PLOS ONE policies on sharing data and materials.

* Email: hiroshiy@med.nagoya-u.ac.jp

Introduction

Cell transplantation, which is a simple, rapid and minimally-invasive method relative to whole organ transplantation, has been demonstrated to be effective for treating various diseases such as diabetes, central nervous system (CNS) disorders and cancers including hematological diseases [1]. In particular, stem cell transplantation has been expected to have applications for regenerative medicine. Tsuji et al. showed that the transplantation of induced pluripotent stem (iPS) cells -derived neurospheres was effective for treating spinal cord injury [2]. Liu et al. showed that the transplantation of a combination of mesenchymal stromal cells and haploidentical hematopoietic stem cells facilitated platelet recovery without increasing the recurrence of leukemia [3]. However, the clinical application of stem cell transplantation for many internal organs has been restricted due to the lack of sufficient technology to trace such transplanted stem cells to confirm their correct implantation and to evaluate their growth and migration *in vivo* [4].

In order to reveal the location and accumulation of transplanted stem cells in various tissues and organs deep in the body, a non-invasive and widely clinically available cell imaging technology is

needed [5,6]. We herein focus on magnetic resonance (MR) imaging as a method for tracing the transplanted stem cells, because it is a non-invasive, irradiation-free and clinically used method offering good tissue contrast [7]. The MR imaging of stem cells is currently an emerging strategy for tracing transplanted stem cells. To increase the contrast of issues in typical imaging studies, MR contrast agents such as gadolinium (Gd) and superparamagnetic iron oxide (SPIO) nanoparticles are generally used [8,9]. These agents cause hydrogen relaxivity changes and induce contrast modifications [8]. In particular, SPIO nanoparticles are known to generate a strong transverse relaxation time T2-negative contrast in MR images and to decrease the signal intensity [10]. In addition, T2-weighted agents including SPIO nanoparticles are preferentially used for cellular MR imaging since they are more biocompatible and more highly magnetic than T1-weighted agents, resulting in higher contrast modification on MR imaging with a lower concentration than T1-weighted agents [8].

Various SPIO nanoparticles have been developed as contrast agents, including ferucarbotran (Resovist), ferumoxide (Feridex, Endorem) and ferumoxtran-10 (Combidex, Sinerem) [11,12]. Ferucarbotran, an anionic SPIO nanoparticle with a carboxydextran coating has been successfully applied in the clinical setting as a liver contrast agent [13]. It was recently reported that ferucarbotran could more efficiency magnetically label stem cells than ferumoxide and ferumoxtran without including cytotoxicity [4,14]. In this study, we also demonstrate that stem cells can be labeled with ATDM which is a major component of ferucarbotran.

A more common method of labeling cells utilizes cationic transfection reagents to induce the formation of complexes with negatively charged SPIO nanoparticles, because positive charges have been generally considered to be effective for accelerating the intracellular incorporation of such particles [15-18]. Several groups have shown that protamine, which is a low molecular weight polycationic peptide approved by the U.S. FDA as an antidote for heparin anticoagulation, enhanced the uptake of ATDM into stem cells [19]. However, they could not form stable complexes with SPIO nanoparticles, and therefore, it is difficult to clarify the influence of these agents on stem cells [20].

In order to overcome these problems, we have developed five novel contrast agents to use for MR imaging; trimethylamino dextran-coated magnetic iron oxide nanoparticles with different positive charges [21,22]. TMADM-03 has proven to be stably dispersed in the culture medium including fetal bovine serum, and is efficient for labeling mature cells without exerting cytotoxic effect. In fact, Min6 cells, which are a β-cell line, could be efficiently labeled with TMADM-03 without signs of cytotoxicity [22,23]. However, the applicability of TMADM-03 for stem cells remains to be elucidated.

In our research group, adipose tissue-derived stem cells (ASCs) have been the major focus as the stem cell source for regenerative medicine, including stem cell transplantation [24]. ASCs can be easily obtained in abundance by minimally invasive harvest procedures, such as lipoaspiration under local anesthesia, and have the ability to differentiate into not only mesenchymal cells, but also epithelial and endothelial cells [25,26]. Moreover, ASCs have already been used for some clinical treatments [27]. ASCs thus are expected to provide a useful and effective source of the stem cells for regenerative medicine, including stem cell transplantation.

In this study, we investigated whether TMADM-03 could efficiently label ASCs without adverse effects, and determined whether the labeled ASCs could be observed *in vitro* and *in vivo* using MR imaging.

Materials and Methods

Materials

ATDM, which is a major component of ferucarbotran (Resovist), and TMADM-03 were provided by Meito Sangyo Co., Ltd. (Nagoya, Japan). The Cell Counting Kit-8 (CCK-8) was purchased from Dojindo Laboratories (Kumamoto, Japan). Iron standard solution (Fe 1000) and LabAssay-triglyceride were purchased from Wako Pure Chemical Industries, Ltd. (Osaka, Japan). Microhomogenizers for 1.5 mL microtubes ((3810)226AG) were purchased from Eppendorf Japan (Tokyo, Japan). Inductively coupled plasma - atomic emission spectrometry (ICP-AES) was employed to measure the iron concentrations. The Adipo-Inducer Reagent and Osteoblast-Inducer Reagent were purchased from Takara Bio. Inc. (Shiga, Japan). The Quantikine Mouse HGF Immunoassay and Quantikine Mouse VEGF Immunoassay were purchased from R&D systems (Minneapolis, USA). The mouse PGE2 ELISA kit was purchased from Cusabio Biotech Co., Ltd. (Wuhan, China). MACS LS column was purchased from Miltenyi Biotech (Tokyo, Japan).

Animals

C57BL/6 mice were purchased from SLC Japan. The mice were housed in a controlled environment (12 h light/dark cycles at 21°C) with free access to water and an alfalfa-free diet before sacrifice. All conditions and handing of animals in this study were conducted under protocols (024–002 and 025–018) approved by the Nagoya University Committee on Animal Use and Care.

Isolation and culture of ASCs

The isolation and culture of ASCs were reported previously [26]. Briefly, ASCs were collected from seven to fourteen-month-old female C57BL/6 mice. The adipose tissues in the inguinal groove were isolated and cut finely, then digested with type II collagenase (Collagenase Type II, Koken Co., Ltd., Tokyo, Japan) at 37°C in a shaking water bath for 90 min. Adipose tissue cells were when suspended in culture medium (Dulbecco's modified Eagle's medium (DMEM)/F12 containing 20% fetal bovine serum (FBS: Trace Scientific Ltd., Melbourne, Australia) and 100 U/mL penicillin/streptomycin). The cells were centrifuged at 1,200 rpm for five minutes at room temperature to obtain a pellet containing the ASCs. The cells were washed three times by suspension and centrifugation in the culture medium. The primary cells were then cultured for four to five days until they reached confluence and were defined as passage "0". The cells used in all of the experiments were between passages two and five.

Cytotoxicity of ATDM and TMADM-03 to ASCs

ASCs (1×10^4) were seeded in a 96-well plate (BD Biosciences) with 100 μL of culture medium for four hours at 37°C, which was then replaced with 100 μL of transduction medium (DMEM/F12 containing 2% FBS and 100 U/mL penicillin/streptomycin). ATDM (5 mg-Fe/mL) and TMADM-03 (5 mg-Fe/mL) were prepared at various concentrations (0, 5, 10, 50 and 100 μg-Fe/mL) with transduction medium, and were added into each well. After a one or 24 h incubation, the cells were counted using the CCK-8. The CCK-8 reagent (10 μL) was added to each well and the reaction was allowed to proceed for up to four hours. The absorbance of each sample at 450 nm was measured against a background control using a microplate reader.

Proliferation of ASCs labeled with TMADM-03

ASCs (2×10^3) were seeded in each well of a 96-well plate with 100 μL of culture medium and were incubated with various

concentrations of TMADM-03. After one hour, the medium was changed to new incubation medium after the cells were washed with PBS three times to eliminate the remaining TMADM-03 in the culture medium. The cells were incubated for two or seven days, and then viable cells were counted using the CCK-8 in the same way as described above.

Electron microscopy analysis

Electron microscopy was used to visualize the presence of TMADM-03 inside the ASCs. ASCs labeled with TMADM-03 were fixed with 2% paraformaldehyde and 2% glutaraldehyde in 0.1 M phosphate buffer (pH 7.4) at 4°C for 24 h, followed by incubation in 2% osmium tetroxide at 4°C for 90 min. The cells were dehydrated in increasing concentrations of ethanol, immersed in propylenoxide and then embedded in Quetol 812 (Nissin EM, Tokyo). Ultrathin sections (70 nm) were stained using Reynold's lead citrate and examined using a JEM-1200EX transmission electron microscope (TEM) (JOEL, Ltd., Tokyo) at an accelerating voltage of 80 kV. These studies were done in cooperation with the Tokai Electron Microscopy Analysis Co., Ltd. (Aichi, Japan).

Quantitative determination of Fe in ASCs labeled with TMADM-03

ASCs (1×10^6) were incubated with ATDM or TMADM-03 at various concentrations (10, 30 and 50 μg-Fe/mL) in transduction medium for one hour. The amount of Fe was measured by phenanthroline spectrophotometric method and ICP-AES method. Briefly, in the ICP-AES method, the ASCs labeled with ATDM or TMADM-03 were washed with PBS three times and were collected by trypsinization. Concentrated nitric acid solution (2 mL) was added to the collected cells, and thermolysis of the solution was conducted at 200°C for four to five hours. After the volatilization of the solution, distilled water was added to the pellets derived from the labeled cells until they weigh 5 g. Next, the Fe concentration of the pellets was measured using the ICP-AES at the analytical wavelength of 259.74 nm. Iron standard solution (Fe 1000) (Wako) was serially diluted, and then used as a standard solution of Fe for comparison purposes.

The labeling efficiency of TMADM-03 for ASCs

The labeled ASCs with TMADM-03 were separated from unlabeled ASCs using MACS LS column in MACS technology according to the manufacture's procedure [28,29]. In brief, ASCs (3×10^5) were labeled with TMADM-03 (0, 10 and 30 μg-Fe/mL) in a one hour incubation, then the ASCs were washed with PBS three times and were collected by the centrifugation at 1200 rpm for 3 min. The ASCs were suspended with transduction medium (2 mL) and the cell suspension was filled into the prerinsed MACS LS column in the magnetic field of the MACS magnet. The ASCs labeled with TMADM-03 were bound to the column, whereas non-labeled ASCs passed through the column. The column was removed and the ASCs labeled with TMADM-03 were released from magnetic field. The column was washed three times with transduction medium (3 mL). The collected cells were counted, and the collected rate was calculated as the labeling efficiency of TMADM-03 for ASCs.

Analysis of the mechanism of TMADM-03 uptake

ASCs (5×10^5) were seeded in each well of a 6-well plate with 2 mL of culture medium and incubated for 24 h at 37°C. The cells were then treated with endocytosis inhibitors, 10 mM sodium azide and 2-deoxy-D-glucose, 5 mM amiloride, 5 μg filipin III, or 12.5 μg chlorpromazine (CPZ) at 37°C for one hour (15 min for amiloride), and then were treated with TMADM-03 (30 μg-Fe/mL) and incubated for one hour at 37°C. In addition, the treatment of incubation at 4°C for one hour was conducted to inhibit endocytosis. Then, the cells were collected and the Fe (II) concentration was measured as described above.

Adipogenic differentiation

The Adipo-Inducer Reagent was used for the adipogenic differentiation of ASCs. Their differentiation was conducted in accordance with the accompanying product manual. Briefly, the differentiation solution was prepared by adding insulin solution (1 mL), dexamethasone solution (0.5 mL) and 3-isobuthyl-1-methylxanthine solution (0.1 mL) into the culture medium (100 mL). The incubation solution was prepared by adding insulin solution (1 mL) into the culture medium (100 mL). ASCs with or without the TMADM-03 label were incubated with the differentiation medium for two days. Thereafter, the medium was exchanged for the incubation medium, then cells were incubated for another five to ten days.

The adipogenic differentiation was confirmed by Oil Red O staining as an indicator of intracellular lipid accumulation. Briefly, the cells were fixed in a 10% solution of formaldehyde in PBS for at least 10 min at room temperature, and then were washed with 60% isopropanol. Next, the cells were stained with 2% (w/v) Oil Red O reagent for 10 min at room temperature, followed by repeated washing with distilled water and destaining in 100% isopropanol for one minute.

Osteogenic differentiation

The Osteoblast-Inducer Reagent was used for the osteogenic differentiation of ASCs as specified by the manufacture's product manual. Briefly, the differentiation solution was prepared by adding ascorbic acid (1 mL), hydrocortisone (0.2 mL) and β-glycerophosphate (1 mL) into the culture medium (100 mL). ASCs with or without the TMADM-03 label were incubated with the differentiation medium for 14 to 21 days. The medium was changed to fresh differentiation medium every seven days.

The osteogenic differentiation was confirmed by staining for alkaline phosphatase activity. The cells were then washed twice with PBS and fixed in 10% formalin for 15 min at room temperature. They were then washed and incubated with deionized water for 15 min, and were subsequently stained with a solution containing naphthol AS MX-PO_4 (Sigma, N-5000), *N*, *N*-dimethylformamide (Wako Pure Chemical Industries Ltd.), Red Violet LB salt (Sigma, F-1625) and Tris-HCl buffer (pH 8.3) for 45 min.

Triglyceride measurement

ASCs (2×10^5) were seeded in each well of a 12-well plate with 2 mL of culture medium and were transduced with TMADM-03 (30 μg-Fe/mL). After the process of adipogenic differentiation, the cells were treated with trypsin and collected into microtubes. PBS (100 μL) was added into the tubes, and then the cells were shredded with microhomogenizers. The amount of triglyceride in the microtubes was measured using the LabAssay Triglyceride Kit according to the manufacture's protocol. Briefly, the color-producing reagent was diluted with buffer solution and the coloring reagent was prepared. The coloring reagent was then added into the samples and standard solutions, and then incubated for five minutes at 37°C. The absorbance at 600 nm was measured by a BioPhotometer (Eppendorf, Tokyo, Japan) and the amount of triglyceride was calculated.

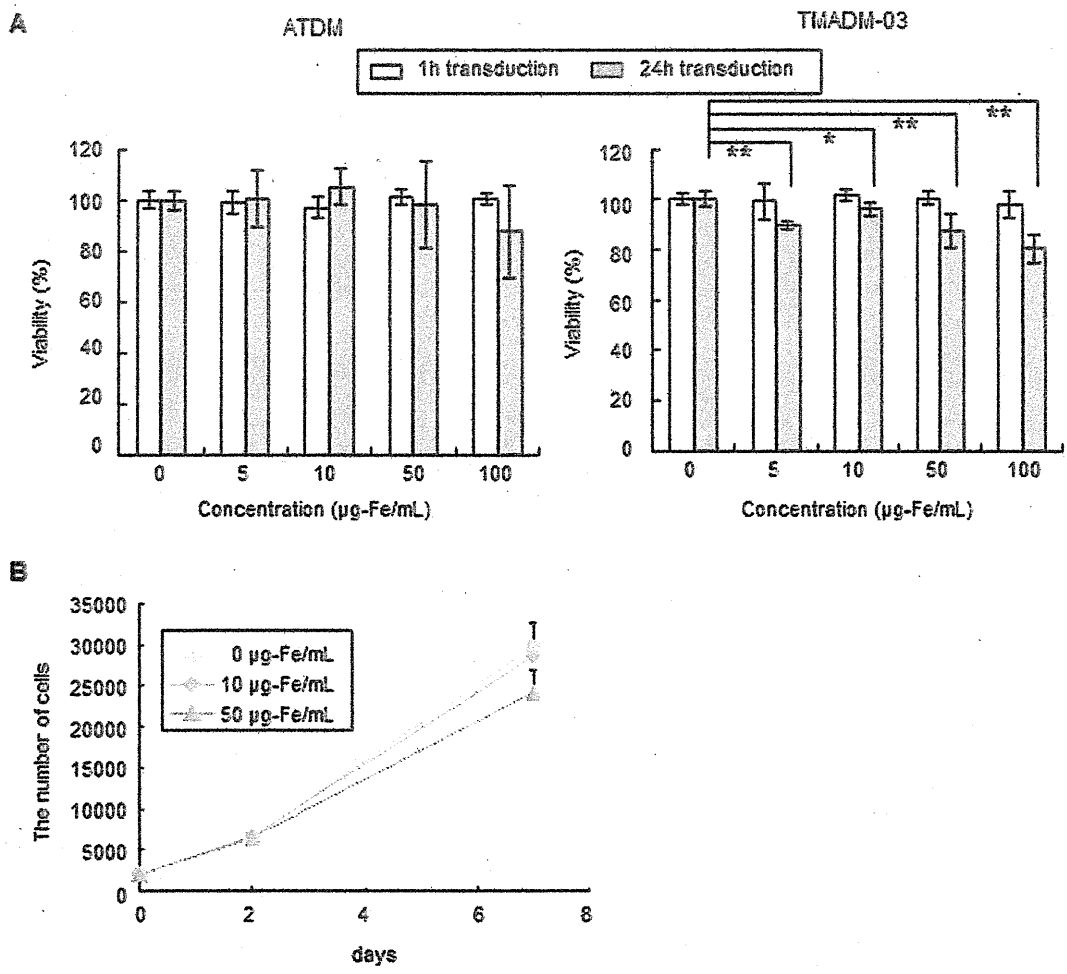

Figure 1. The viability and proliferation rate of ASCs labeled with ATDM or TMADM-03. A: The viability of ASCs labeled with ATDM or TMADM-03 (0, 5, 10, 50, 100 μg-Fe/cell) after a 1 h (white bars) or 24 h (gray bars) transduction at 37°C. There were significant differences in the viability of ASCs labeled with TMADM-03 after the 24 h transduction. B: The proliferation rate of ASCs labeled with TMADM-03 (0, 10, 50 μg-Fe/mL) at 0, 2 and 7 days after 1 h transduction. No significant differences were observed at any of the concentrations of TMADM-03. These data are shown as the means ± standard deviation of triplicate values. *$P<0.05$. **$P<0.01$.
doi:10.1371/journal.pone.0110142.g001

Quantitative estimation of alkaline phosphatase expression

ASCs (1×10^5) were seeded in each well of a 24-well plate with 1 mL of culture medium, and were transduced with TMADM-03 (30 μg-Fe/mL). After the process of osteogenic differentiation, the alkaline phosphatase expression was evaluated by measuring the alkaline phosphatase staining area.

Enzyme-linked immunosorbent assays

ASCs (1×10^5) were seeded into each well of a 24-well plate, and were transduced with TMADM-03 (30 μg-Fe/mL) for one hour. Then, the cells were washed with culture medium, and incubated in fresh culture medium for 24 or 72 h at 37°C. The culture supernatants were collected, and then the levels of mouse HGF, VEGF and PGE2 produced by the ASCs labeled with TMADM-03 and non-labeled ASCs (Normal) in the medium were measured using specific ELISA kits according to the manufacturer's protocols.

ASCs transplantation

ASCs were labeled with TMADM-03 (30 μg-Fe/mL) for 1 h at 37°C. At the end of the uptake experiments, the ASCs were washed three times in the transduction medium, and were collected in microtubes. The ASCs (1×10^6) were transplanted into the renal subcapsular space of the right kidney of a mouse. Moreover, the ASCs (2×10^6) labeled with TMADM-03 (30 μg-Fe/mL) as the same condition were subcutaneously transplanted on the back of the mouse for *in vivo* imaging.

MR imaging

The mice were lightly anesthetized using isoflurane (3% induction and 1.5% maintenance) prior to imaging. MR imaging data were collected on a 1T MRI (MRTechnology, Tsukuba, Japan) according to the manufacture's procedure. In brief, the imaging parameters were as follows: T2 sequences with a TR/TE of 3000/69 ms, field of view (FOV): 30 and two averages were taken for a total acquisition time of about 14 min. T1 sequences were composed of a TR/TE of 500/9 ms, FOV: 30 and four

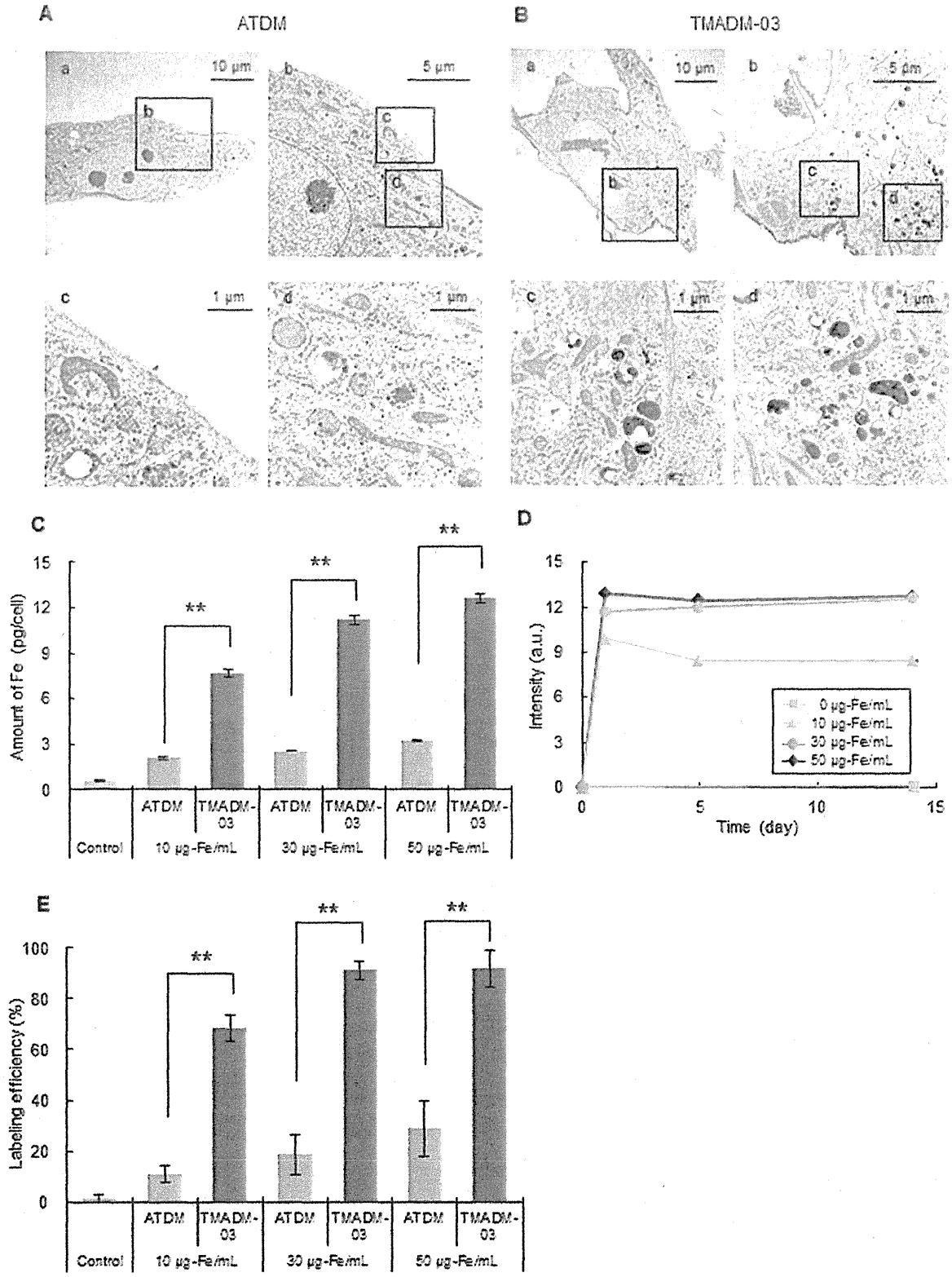

Figure 2. Confirmation of the uptake of ATDM and TMADM-03 by ASCs. A: The images obtained by transmission electron microscopy of ASCs labeled with ATDM (30 μg-Fe/mL) for 1 h at 37°C (a–d). A picture of the cells labeled with ATDM is shown (a). The surface of the cells labeled with ATDM is shown (b). The aggregates of the ATDM internalized by ASCs are shown by yellow arrows in (c) and (d). B: The images obtained by transmission electron microscopy of ASCs labeled with TMADM-03 (30 μg-Fe/mL) for 1 h at 37°C (a–d). A picture of the cells labeled with TMADM-03

is shown (a). The surface of the cells labeled with TMADM-03 is shown (b). The aggregates of the TMADM-03 internalized into ASCs are shown by yellow arrows in (c) and (d). The amount of TMADM-03 internalized in the cytoplasm of ASCs was found to be much higher than that of ATDM. C: The results of the quantitative determinations of the ATDM and TMADM-03 (10, 30, and 50 μg-Fe/mL) internalized into ASCs after a 1 h transduction by measuring the concentration of Fe derived from ATDM or TMADM-03 using ICP-AES. The control (Cont.) shows the amount of Fe normally in ASCs, without labeling by nanoparticles. Significant differences between ATDM and TMADM-03 were confirmed after the transduction at all concentrations. These data are shown as the means ± standard deviation of triplicate values. $^{**}P<0.01$. D: The changes in the amount of TMADM-03 (0, 10, 30 and 50 μg-Fe/mL) internalized by ASCs after a 1 h transduction for two weeks. The data are shown as the means ± standard deviation of triplicate values. E: The labeling efficiency of TMADM-03 (0, 10, 30 and 50 μg-Fe/mL) for ASCs after a 1 h transduction using MACS Technology.
doi:10.1371/journal.pone.0110142.g002

averages for a total acquisition time of about five minutes. All T1 and T2 -weighted image data sets were visually evaluated to identify the location of the transplanted cells within each animal.

Prussian blue (PB) staining

The existence of iron particle (TMADM-03) within tissues was confirmed by the PB staining which is a traditional method for detecting the iron (ferric form) according to the manufacture's procedure [30,31]. In brief, the hydrochloric acid and potassium ferrocyanide were mixed and prepared immediately before use. The slides were immersed in this solution for 20 min, and then washed in distilled water three times. Next, the slides were treated with counterstain solution with for 5 minutes, and the slides were rinsed twice in distilled water. Then, the slides were dehydrated through 95% to 100% alcohol, and cleared in xylene two times for 3 minutes each. The slides were covered with resinous mounting medium.

Statistical analysis

Numerical values are presented as the means ± SD. Each experiment was repeated three times. The statistical significance was evaluated using unpaired Student's *t*-tests for comparisons between two groups; p-values <0.05 were considered to be statistically significant. All statistical analyses were performed using the SPSS software package.

Results

Cytotoxicity of ATDM and TMADM-03 to ASCs

ATDM and TMADM-03 were transduced into ASCs at various concentrations in transduction medium for one or 24 h incubations. Cytotoxicity was observed in the ASCs transduced for 24 h at all concentrations of TMADM-03, however, the degree of cytotoxicity was slight, and more than about 80% of the cells were still alive after the treatment. In addition, no cytotoxicity was observed after a one hour incubation at all concentrations of TMADM-03. On the other hand, no cytotoxicity of ATDM was observed under all of these experimental conditions (Fig. 1A).

Next, the influence of the compounds on the proliferation rate was examined for the non-cytotoxic conditions with TMADM-03. The cells were confirmed to exhibit a logarithmic growth rate that was nearly equal to that of normal, un-treated, ASCs. No significant differences were observed under these conditions (Fig. 1B). These data suggest that TMADM-03 could be used to label cells for one hour at a 100 μg-Fe/mL concentration.

Observation of ATDM and TMADM-03 internalization inside ASCs

To detect the internalization of ATDM and the TMADM-03 internalization by ASCs, the cells were transduced with 30 μg-Fe/mL of ATDM or TMADM-03 by a one hour incubation. The SPIO nanoparticles could be observed in ASCs transduced with both ATDM and TMADM-03 using TEM, and these nanoparticles were found in the cell cytoplasm and lysosomes. However, the degree of TMADM-03 incorporation was remarkably higher than that of ATDM (Figs. 2A, B), In addition, as shown in Fig. 2B-b, the surface of ASCs was found to be covered with TMADM-03. These data suggest that both ATDM and TMADM-03 could be transduced into ASCs within one hour of incubation, but the efficiency was markedly higher for TMADM-03.

Comparison of the uptake of ATDM and TMADM-03 by ASCs

To measure the uptake of ATDM and TMADM-03 by ASCs, the amount of Fe derived from ATDM and TMADM-03 in ASCs

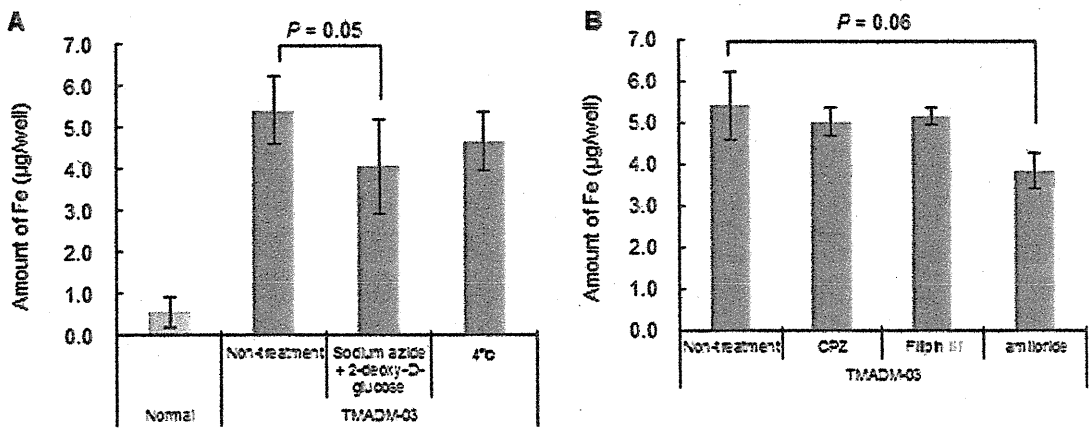

Figure 3. The mechanism of uptake of TMADM-03 by ASCs. A: The effect of endocytosis inhibitors on TMADM-03 internalization in ASCs. Cells were treated with sodium azide and 2-deoxy-D-glucose, or incubated at 4°C. B: The effect of pinocytosis inhibitors on TMADM-03 internalization in ASCs. Cells were treated with chlorpromazine (CPZ), Filipin III, or amiloride. The data are shown as the means ± standard deviation of triplicate values.
doi:10.1371/journal.pone.0110142.g003

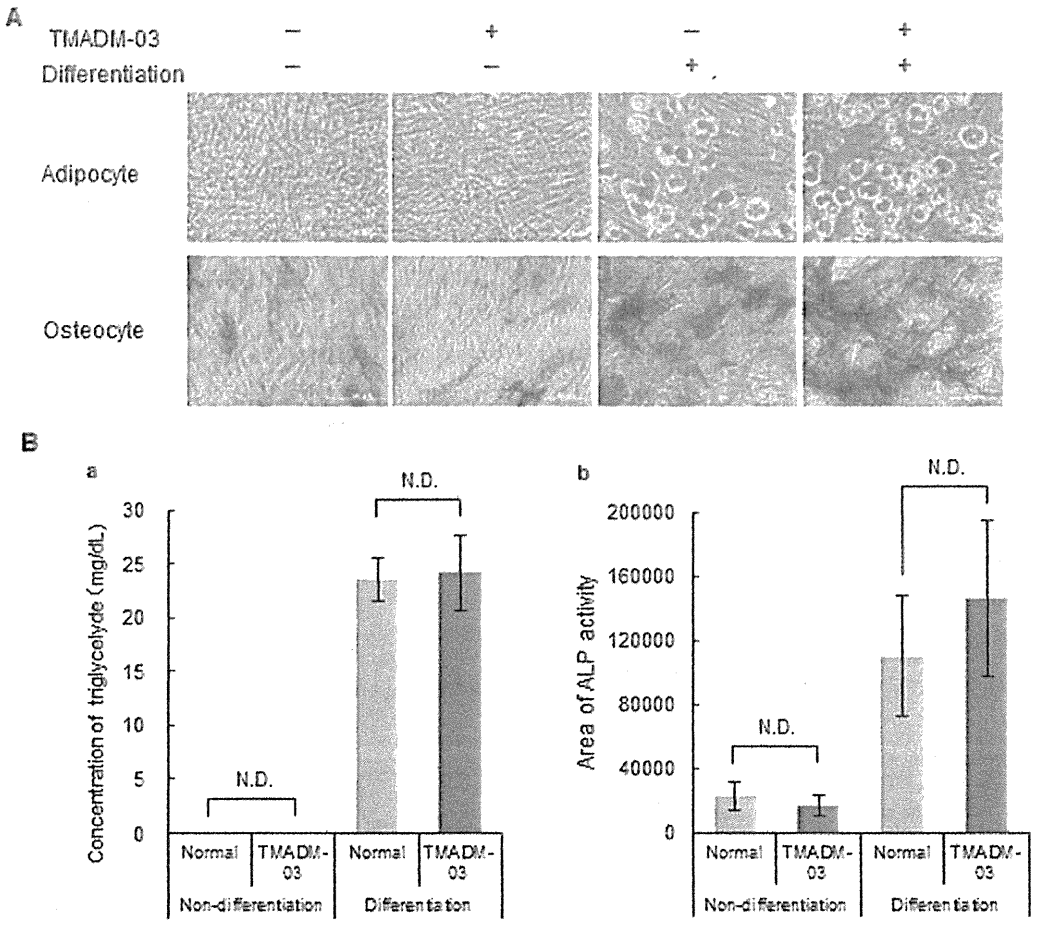

Figure 4. The differentiation capacity of ASCs labeled with TMADM-03. A: The ability of unlabeled ASCs or those labeled with TMADM-03 (30 μg-Fe/mL) to differentiate into adipocytes and osteocytes. The extent of adipogenic differentiation was assessed by Oil Red O staining. Red spherical bodies in the upper figures show lipid droplets produced by the differentiated ASCs (upper). The extent of osteogenic differentiation was assessed by ALP staining. Purple sites in the lower figures show the ALP produced by the differentiated ASCs (lower). B: The degree of differentiation into adipocytes by the concentration (mg/mL) of triglyceride present in the cells (a). The degree of differentiation into osteocytes by the ALP staining area (b). The data are shown as the means ± standard deviation of triplicate values.
doi:10.1371/journal.pone.0110142.g004

was measured using ICP-AES. The amount of Fe was increased in a concentration-dependent manner for both types of nanoparticles. However, the amount of Fe in cells incubated with TMADM-03 was significantly higher (about four-fold) in comparison to that of ATDM at all concentrations (Fig. 2C). The amount of TMADM-03 was confirmed to remain approximately equal for at least 14 days in 30 and 50 μg-Fe/mL labeling conditions (Fig. 2D). In addition, the labeling efficiency was measured by MACS technology, and the efficiency of TMADM-03 was much higher than that of ATDM at all concentrations. Especially, the labeling efficiency of TMADM-03 in 30 and 50 μg-Fe/mL showed more than 90% (Fig. 2E). These data suggest that ASCs could be efficiently labeled with TMADM-03 at the concentration of 30 μg-Fe/mL and maintained the labeling state for at least 14 days.

Mechanism of TMADM-03 uptake by ASCs

To verify the mechanism of uptake of TMADM-03 in ASCs, the cells were treated with endocytosis inhibitors such as sodium azide and 2-deoxy-D-glucose (endocytosis inhibitors), amiloride (an inhibitor of the Na^+/H^+ exchanger required for macropinocytosis), filipin III (an inhibitor of caveolae formation) or chlorpromazine (CPZ: an inhibitor of AP-2-mediated clathrin-coated pit formation) at 37°C for one hour (15 min for amiloride). In addition, treatment by incubation at 4°C for one hour was also employed to inhibit endocytosis. The transduction of TMADM-03 was inhibited by the incubation at 4°C and the treatments with sodium azide and 2-deoxy-D-glucose, or amiloride (Figs. 3A, B). These data suggest that the uptake of TMADM-03 into ASCs was mainly dependent on the endocytosis, particularly macropinocytosis.

Differentiation of ASCs labeled with TMADM-03

To exam the influence of TMADM-03 on the differentiation capacityof ASCs, normal (non-labeled) and labeled ASCs were differentiated into adipocytes or osteoblasts, and then the degree of differentiation in the non-labeled and labeled ASCs was quantitatively compared. The differentiation of ASCs after treatment with TMADM-03 into either adipocytes or osteocytes was observed. There were also no significant differences between the

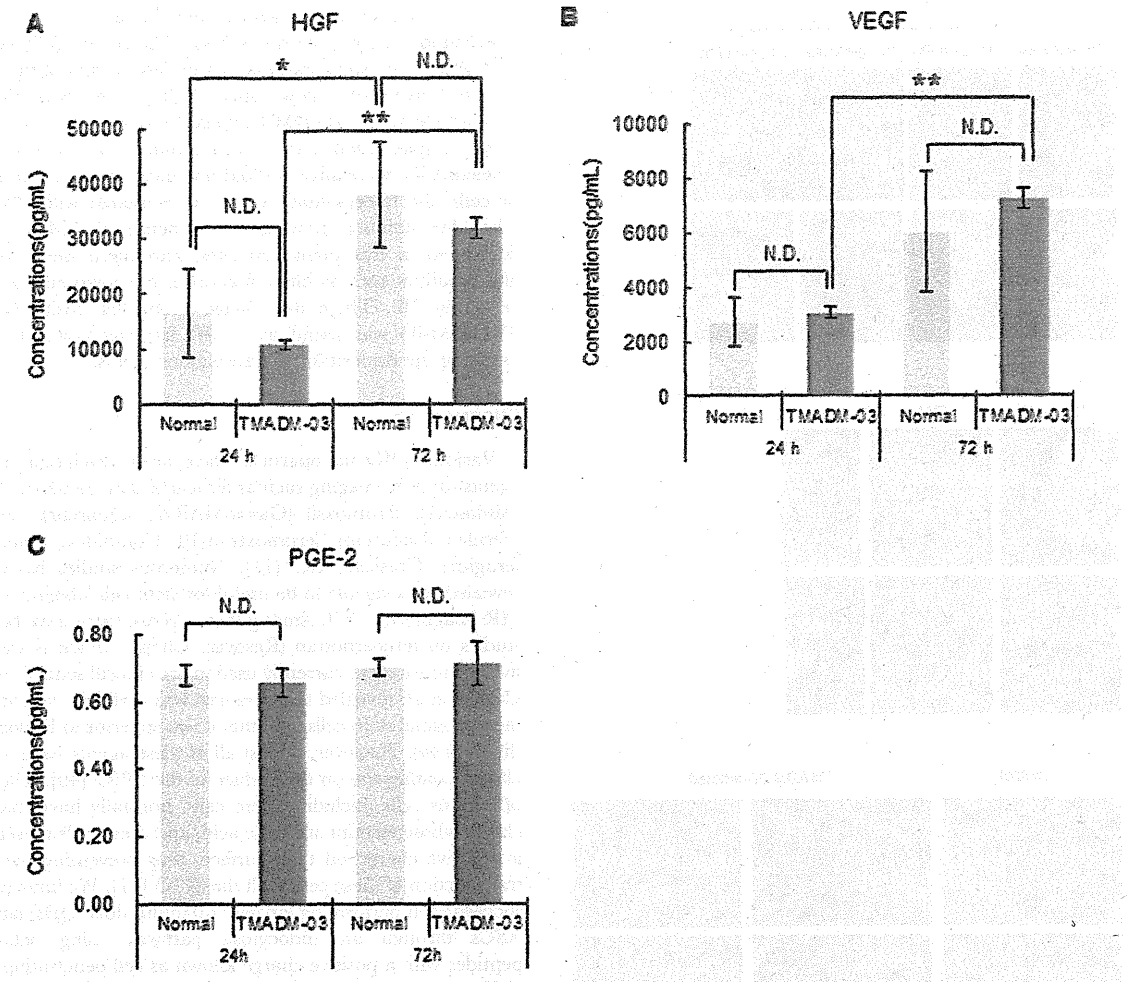

Figure 5. The levels of cytokines produced by ASCs labeled with TMADM-03. A: The concentration of HGF produced by non-labeled (normal) ASCs (1×10^5) or ASCs labeled with TMADM-03 incubated for 24 and 72 h in the culture medium. B: The concentration of VEGF produced by non-labeled (normal) ASCs (1×10^5) or ASCs labeled with TMADM-03 incubated for 24 and 72 h in the culture medium. C: The concentration of PGE2 produced by non-labeled (normal) ASCs (1×10^5) or ASCs labeled with TMADM-03 incubated for 24 and 72 h in the culture medium. The data are shown as the means ± standard deviation of triplicate. *$P<0.05$, **$P<0.01$.
doi:10.1371/journal.pone.0110142.g005

non-labeled and labeled ASCs in terms of the concentration of triglycerides, indicating the degree of adipogenic differentiation (Figs. 4A, B–a). Moreover, similar expression of ALP indicating the degree of osteogenic differentiation was confirmed in the cells incubated with and without the TMADM-03 (Figs. 4A, B–b). These data suggest that TMADM-03 does not affect the differentiation of ASCs.

Cytokine production from ASCs labeled with TMADM-03

To confirm the production of HGF, VEGF and PGE2 from non-labeled ASCs or ASCs labeled with TMADM-03, the levels of these cytokines in the culture medium from ASCs cultured for 24 or 72 h were measured using specific ELISA kits. The production of these cytokines could be confirmed in both non-labeled and labeled ASCs, and no significant differences were observed in the production of any of these cytokines (Fig. 5). These data raised the possibility that the ability of ASCs to produce cytokines could be maintained after labeling with TMADM-03.

In vitro MRI of ASCs labeled with TMADM-03

To examine whether the cells labeled with 10, 30 and 50 μg-Fe/mL of TMADM-03 could be detected by MR imaging, the labeled cells (1×10^6) were collected in PBS and spun down, then the cell pellet was prepared for the MR analysis in microtubes. The labeled cell pellet could be detected at a lower intensity on both T1 and T2-weighted images in comparison to the unlabeled cell pellet (Fig. 6A). These results suggested that the cells labeled with more than 30 μg-Fe/mL of TMADM-03 could be detected with sufficient contrast for cell visualization by MR imaging.

MR imaging of ASCs labeled with TMADM-03 in mice

To assess whether images of transplanted ASCs labeled with TMADM-03 could be obtained in mice, the ASCs (1×10^6) labeled with 30 μg-Fe/mL of TMADM-03 after a one hour incubation were transplanted into the left kidney capsule of a mouse. The MR imaging data of both cross-section figures from the back and head three hour after transplantation showed remarkable decreases in signal intensity on T1 and T2-weighted images at the implanted

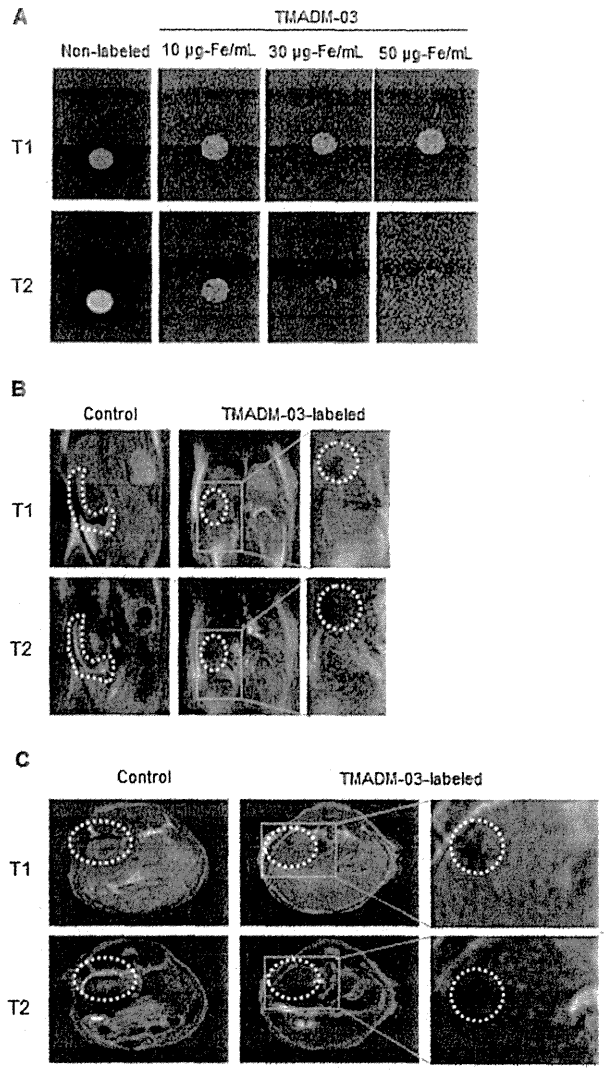

Figure 6. MR imaging of ASCs labeled with TMADM-03 in the kidney capsule. A: *In vitro* MR imaging of unlabeled and labeled ASCs (1×10^6). T1- (upper) and T2- (lower) weighted images were obtained for unlabeled ASCs and for ASCs labeled with TMADM-03 (10, 30 and 50 μg-Fe/mL). B: *In vivo* MR imaging of unlabelled ASCs (1×10^6) or the same number of ASCs labeled with TMADM-03 (30 μg-Fe/mL) in a cross-section figure from the back of the mouse. T1- (upper) and T2- (lower) weighted images were obtained for unlabeled ASCs, and for ASCs labeled with TMADM-03 3 hours after transduction. Yellow dotted circles show the transplanted ASCs. C: *In vivo* MR imaging of unlabeled ASCs (1×10^6) or the same number of ASCs labeled with TMADM-03 (30 μg-Fe/mL) in a cross-section figure from the head of the mouse. T1- (upper) and T2- (lower) weighted images were obtained for unlabeled ASCs and for ASCs labeled with TMADM-03. The yellow dotted circles show the transplanted ASCs. These images were obtained using a 1T MRI instrument (MR Technology).
doi:10.1371/journal.pone.0110142.g006

site in the left kidney of a mouse that was transplanted with ASCs labeled with TMADM-03. On the other hand, in a mouse transplanted with unlabeled ASCs, no decrease in the signal intensity on T2 was observed in the MR imaging results (Figs. 6B C).

In addition, to investigate whether the labeled ASCs could be detected for 14 days, the ASCs (2×10^6) labeled with 30 μg-Fe/mL of TMADM-03 were transplanted under the skin of the back of a mouse at two sites (yellow dotted circles). The ASCs labeled with 30 μg-Fe/mL of TMADM-03 could be traced for at least 14 days after transplantation (Fig. 7A). In addition, to reveal whether the labeled ASCs were alive and did not affect the surrounding tissues or cells, the transplantation sites were treated with PB staining. The blue staining showing the existence of TMADM-03 was confirmed in transplantation sites, and there were no obvious abnormalities such as inflammation in the surrounding tissues or cells (Fig. 7B). These data suggest that the positively charged TMADM-03 was useful as a MR imaging contrast agent for assessing the disposition of transplanted ASCs.

Discussion

Various SPIO nanoparticles have been developed as contrast agents for MR imaging such as ferucarbotran (Resovist), ferristene (Abdoscan), ferumoxsil (GastroMARK, Lumirenr), ferumoxide (Feridex, Endorem), ferumoxtran-10 (Combidex, Sinerem) and feruglose (Crasican) etc. [11]. Numerous studies have recently revealed these agents to be useful for stem cell labeling for *in vivo* MR imaging [32–37]. Among these agents, there have been many studies on ferucarbotran (Resovist, Clivist), which is well known liver contrast agent currently used in the clinical setting [10,38,39]. Crabbe et al. revealed that Resovist was useful for labeling mouse mesenchymal stem cells, and that it was superior to Endoderm and Sinerem [4]. However, almost all of these agents have a negative charge coating site on the surface of the SPIO [40]. The surfaces of various cells, including stem cells, normally have many sugar chains whose termini are sialic acid, and these cells therefore have a negative charge on their surface, thus preventing the effective transduction of these cells with the SPIO [41]. We have previously succeeded in performing efficient quantum dots (QDs) labeling for ASCs through an endocytosis pathway using octa-arginine peptides with a positive charge known as cell penetrating peptides (CPPs) [42]. Various CPPs have been identified including the third helix of the homeodomain of antennapedia [43,44], VP22 herpesvirus protein [45] and the HIV-Tat protein [46]. Most of these peptides have a positive charge derived from amino acids such as arginine and lysine. In this study, we demonstrated that TMADM-03, which has a positive charge, can label ASCs more efficiently than ATDM which is a major component of ferucarbotran that has a negative charge.

We have already reported that the zeta voltages of ATDM and TMADM-03 were -15 mV and +2.0 mV, respectively [23]. When ASCs were transduced with TMADM-03 during a one hour incubation, the surface of ASCs was observed to be covered with TMADM-03 by a TEM analysis. The successful uptake of TMADM-03 by the ASCs was therefore thought to have occurred. The same phenomenon was not found in the case of ATDM. ATDM was thought to incidentally come into contacted with the surface of ASCs, and to subsequently be incorporated into the ASCs. As a result, about a four-fold higher uptake of TMADM-03 in comparison to ATDM was observed by ICP-AES in the present day. According to previous reports, positively charged substrates, such as protamine, can effectively increase the efficiency of transduction of magnetic nanoparticles into cells. Huang et al. reported that an approximately two-fold higher uptake of ATDM was observed when it was complexed with protamine in comparison to the uptake of ATDM alone [39]. In addition, Balakumaran reported that labeling by ferumoxide complexed with protamine did not affect the stemness of bone marrow

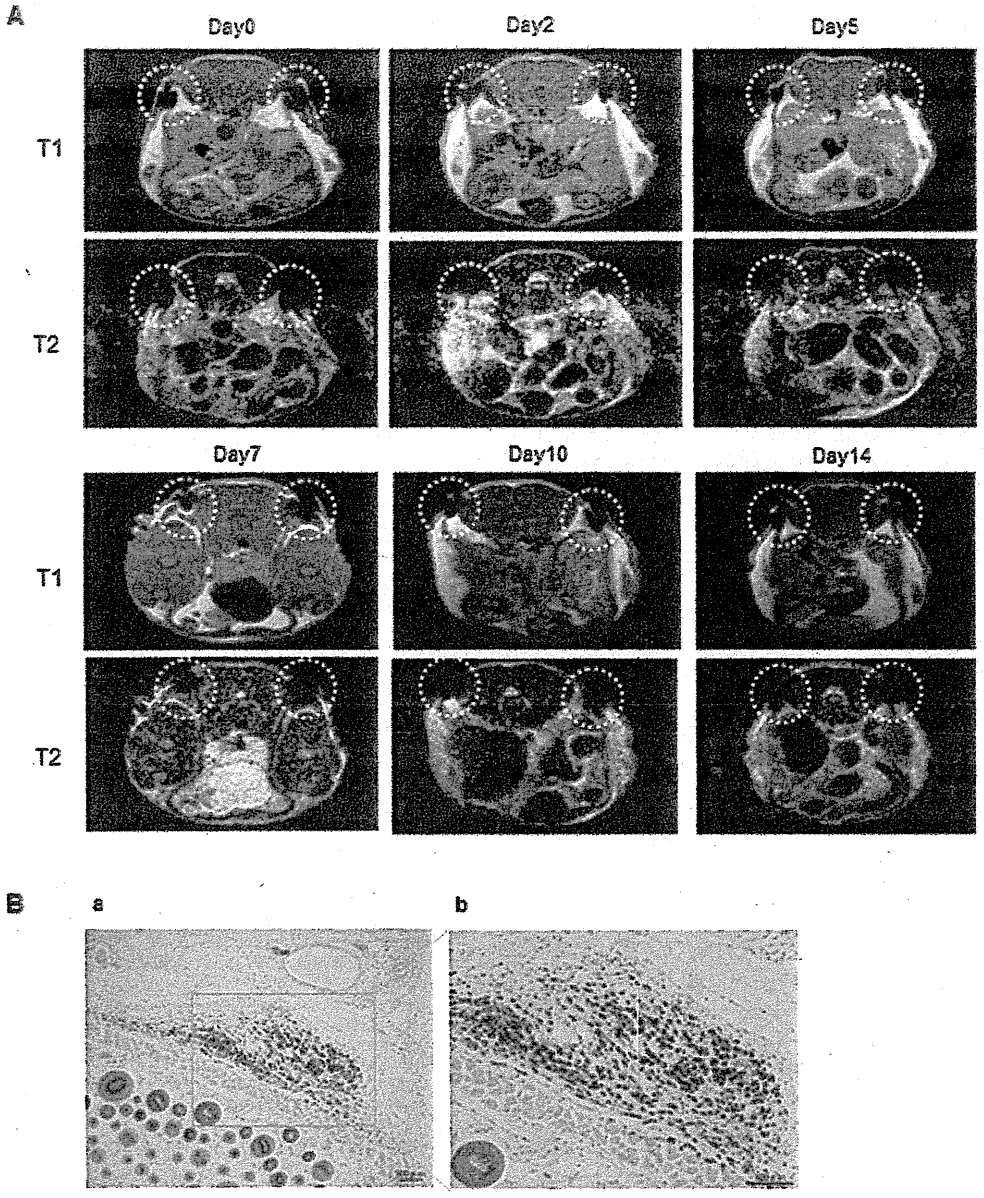

Figure 7. MR imaging of ASCs labeled with TMADM-03 under the skin and Prussian blue staining. A: *In vivo* MR imaging of ASCs (2×10^6) labeled with TMADM-03 (30 μg-Fe/mL) under the skin in a cross-section figure from the head of the mouse for 14 days. The two yellow dotted circles show the transplanted ASCs labeled with 30 μg-Fe/mL of TMADM-03. These images were obtained using a 1T MRI instrument (MR Technology). B: Prussian blue staining of the transplanted ASCs labeled with TMADM-03.
doi:10.1371/journal.pone.0110142.g007

mesenchymal stem cells [34]. However, the efficiency of uptake of ATDM complexed with protamine is assumed to be lower than that of TMADM-03, and the influence of the released protamine on other types of stem cells remains unclear.

Slight cytotoxicity was observed in ASCs transduced with TMADM-03 during a 24 h incubation. However, no cytotoxicity was observed after one hour of incubation at a concentration of up to 100 μg/mL of TMADM-03, and the ASCs labeled with TMADM-03 under these non-cytotoxic conditions exhibited growth equivalent to that of normal ASCs, and could be successfully detected by MRI. The capacity of these cells to differentiate in adipocytes and osteocytes was not affected, and the ability of labeled ASCs to produce cytokines such as HGF, VEGF and PGE2, which are thought to be important for regenerative effects, was maintained after the labeling with TMADM-03. Moreover, the transduction of TMADM-03 into ASCs was inhibited by sodium azide and 2-deoxy-D-glucose (endocytosis inhibitors), and amiloride (a macropinocytosis inhibitor). Although the uptake mechanism of TMADM-03 had previously been unknown, our data indicate that the uptake pathway of TMADM-03 is thought to be mainly dependent on the endocytosis, partially macropinocytosis. These data suggest that TMADM-03 can be a safe and efficient MR contrast agent that can be used to label stem cells for clinical applications.

Using a 1T MR imaging system for small animals, we demonstrated that the ASCs labeled with TMADM-03 could be detected both *in vitro* and *in vivo*. As shown in Fig. 6A, the MR images of the pellet of ASCs labeled with TMADM-03 in a microtube had low signal, and a negative contrast effect could be confirmed. When ASCs labeled with TMADM-03 were transplanted under the skin and the left kidney capsule of a mouse, a negative effect on T2-weighted contrast images could be detected when TMADM-03 was used (Figs. 6B, 6C, 7A). Furthermore, the inflammatory state such as induced by the cell death could not be observed in the surrounding area of the transplantation of ASCs labeled with TMADM-03. These data suggest that TMADM-03 can be used as a contrast agent both *in vitro* and *in vivo* for the MR imaging of stem cells, and raise the possibility that TMADM-03 can provide insights into the location and accumulation of transplanted stem cells in tissues or organs deep in the body.

In conclusion, we investigated whether TMADM-03, which was previously developed by our group, could be used to label ASCs as a MR imaging contrast agent. No cytotoxicity was observed in the ASCs transduced with a concentration of up to 100 μg-Fe/mL of TMADM-03 for a one hour transduction time. The transduction efficiency of TMADM-03 into ASCs was about four-fold higher than that of ATDM, which is a major component of ferucarbotran (Resovist), a clinically-used contrast agent. Of note, the labeling level was maintained for at least two weeks. ASCs labeled with TMADM-03 were confirmed to be able to differentiate into both adipocytes and osteocytes to the same extent as non-labeled ASCs. In addition, the ability of ASCs labeled with TMADM-03 to product cytokines (HGF, VEGF and PGE2) was maintained. The ASCs labeled with TMADM-03 could be imaged with good contrast using a 1T MR imaging system when the labeled ASCs were transplanted into the left kidney capsule of a mouse. Together, these data suggest that TMADM-03 can be utilized as a MR imaging contrast agent for tracking transplanted stem cells.

Acknowledgments

This research is supported by the Japan Science and Technology Agency (JST) through its "Research Center Network for Realization of Regenerative Medicine." We appreciate the help of Naoko Kawakita (Nagoya University) for the treatment of ASCs and the cell labeling. We would also like to thank Tokai Electron Microscopy, Inc. for the technical assistance in the transmission electron microscope observation.

Author Contributions

Conceived and designed the experiments: HY. Performed the experiments: HY SN YY MW HS K. Oishi K. Ono MO YH. Analyzed the data: HY SN YY MW K. Ono DO. Contributed reagents/materials/analysis tools: HS YM HN MS IK NK TI SH YB. Wrote the paper: HY.

References

1. Bhirde A, Xie J, Swierczewska M, Chen X (2011) Nanoparticles for cell labeling. Nanoscale 3: 142–153.
2. Tsuji O, Miura K, Okada Y, Fujiyoshi K, Mukaino M, et al. (2010) Therapeutic potential of appropriately evaluated safe-induced pluripotent stem cells for spinal cord injury. Proc Natl Acad Sci USA 107: 12704–12709.
3. Liu K, Chen Y, Zeng Y, Xu L, Liu D, et al. (2011) Coinfusion of mesenchymal stromal cells facilitates platelet recovery without increasing leukemia recurrence in haploidentical hematopoietic stem cell transplantation: a randomized, controlled clinical study. Stem Cells Dev 20: 1679–1685.
4. Crabbe A, Vandeputte C, Dresselaers T, Sacido AA, Verdugo JM, et al. (2010) Effects of MRI contrast agents on the stem cell phenotype. Cell Transplant 19: 919–936.
5. Son KR, Chung SY, Kim HC, Kim HS, Choi SH, et al. (2010) MRI of magnetically labeled mesenchymal stem cells in hepatic failure model. World J Gastroenterol 16: 5611–5615.
6. Kim HM, Lee H, Hong KS, Cho MY, Sung MH, et al. (2011) Synthesis and high performance of magnetofluorescent polyelectrolyte nanocomposites as MR/near-infrared multimodal cellular imaging nanoprobes. ACS Nano 5: 8230–8240.
7. Tseng CL, Shih IL, Stobinski L, Lin FH (2010) Gadolinium hexanedione nanoparticles for stem cell labeling and tracking via magnetic resonance imaging. Biomaterials 31: 5427–5435.
8. Lalande C, Miraux S, Derkaoui SM, Mornet S, Bareille R, et al. (2011) Magnetic resonance imaging tracking of human adipose derived stromal cells within three-dimensional scaffolds for bone tissue engineering. Eur Cell Mater 21: 341–354.
9. Kim T, Momin E, Choi J, Yuan K, Zaidi H, et al. (2011) Mesoporous silica-coated hollow manganese oxide nanoparticles as positive T1 contrast agents for labeling and MRI tracking of adipose-derived mesenchymal stem cells. J Am Chem Soc 133: 2955–2961.
10. Chen R, Yu H, Jia ZY, Yao QL, Teng GJ (2011) Efficient nano iron particle-labeling and noninvasive MR imaging of mouse bone marrow-derived endothelial progenitor cells. Int J Nanomedicine 6: 511–519.
11. Rosen JE, Chan L, Shieh DB, Gu FX (2010) Iron oxide nanoparticles for targeted cancer imaging and diagnostics. Nanomedicine 8: 275–290.
12. Patel D, Kell A, Simard B, Xiang B, Lin HY, et al. (2011) The cell labeling efficacy, cytotoxicity and relaxivity of copper-activated MRI/PET imaging contrast agents. Biomaterials 32: 1167–1176.
13. Bae JE, Huh MI, Ryu BK, Do JY, Jin SU, et al. (2011) The effect of static magnetic fields on the aggregation and cytotoxicity of magnetic nanoparticles. Biomaterials 32: 9401–9414.
14. Mailänder V, Lorenz MR, Holzapfel V, Musyanovych A, Fuchs K, et al. (2008) Carboxylated superparamagnetic iron oxide particles label cells intracellularly without transfection agents. Mol Imaging Biol 10: 138–146.
15. Bulte JW, Kraitchman DL (2004) Iron oxide MR contrast agents for molecular and cellular imaging. NMR Biomed 17: 484–499.
16. Thorek DL, Tsourkas A (2008) Size, Charge and concentration dependent uptake of iron oxide particles by non-phagocytic cells. Biomaterials 29: 3583–3590.
17. Liu G, Tian J, Liu C, Ai H, Gu Z, et al. (2009) Cell labeling efficiency of layer-by-layer self-assembly modified silica nanoparticles. J Mat Res 24: 1317–1321.
18. Sponarová D, Horák D, Trchová M, Jendelová P, Herynek V, et al. (2011) The use of oligoperoxide-coated magnetic nanoparticles to label stem cells. J Biomed Nanotechnol 7: 384–394.
19. Bull BS, Huse WM, Brauer FS, Korpman RA (1975) Heparin therapy during extracorporeal circulation. II. the use of a dose-response curve to individualize heparin and protamine dosage. J Thorac Cardiovasc Surg 69: 685–689.
20. Arbab AS, Yocum GT, Wilson LB, Parwana A, Jordan EK, et al. (2004) Comparison of transfection agents in forming complexes with ferumoxides, cell labeling efficiency, and cellular viability. Mol Imaging 3: 24–32.
21. Oishi K, Noguchi H, Saito H, Yukawa H, Miyamoto Y, et al. (2010) Cell labeling with a novel contrast agent of magnetic resonance imaging. Cell Transplant 19: 887–892.
22. Oishi K, Noguchi H, Saito H, Yukawa H, Miyamoto Y, et al. (2012) Novel positive-charged nanoparticles for efficient magnetic resonance imaging of islet transplantation. Cell Medicine 3: 43–49.
23. Oishi K, Miyamoto Y, Saito H, Murase K, Ono K, et al. (2013) In vivo imaging of transplanted islets labeled with a novel cationic nanoparticle. PLoS One 8: e57046.
24. Yukawa H, Noguchi H, Oishi K, Takagi S, Hamaguchi M, et al. (2009) Cell transplantation of adipose tissue-derived stem cells in combination with heparin attenuated acute liver failure in mice. Cell Transplant 18: 601–609.
25. Oishi K, Noguchi H, Yukawa H, Miyazaki T, Kato R, et al. (2008) Cryopreservation of mouse adipose tissue-derived stem/progenitor cells. Cell Transplant 17: 35–41.
26. Yukawa H, Noguchi H, Oishi K, Miyazaki T, Kitagawa Y, et al. (2008) Recombinant sendai virus-mediated gene transfer to adipose tissue-derived stem cells (ASCs). Cell Transplant 17: 43–50.
27. Traktuev DO, Merfeld-Clauss S, Li J, Kolonin M, Arap W, et al. (2008) A population of multipotent CD34-positive adipose stromal cells share pericyte and mesenchymal surface markers, reside in a periendothelial location, and stabilize endothelial networks. Circ Res 102: 77–85.
28. Pierzchalski A, Mittag A, Bocsi J, Tarnok A (2013) An innovative cascade system for simultaneous separation of multiple cell types. PLoS One 8: e74745.
29. Kazemi T, Asgarian-Omran H, Hojjat-Farsangi M, Shabani M, Memarian A, et al. (2008) Fc receptor-like 1–5 molecules are similarly expressed in progressive and indolent clinical subtypes of B-cell chronic lymphocytic leukemia. Int J Cancer 123: 2113–2119.
30. Zhang B, Yang B, Zhai C, Jiang B, Wu Y (2013) The role of exendin-4-conjugated superparamagnetic iron oxide nanoparticles in beta-cell-targeted MRI. Biomaterials 34: 5843–5852.
31. Tai JH, Foster P, Rosales A, Feng B, Hasilo C, et al. (2006) Imaging islets labeled with magnetic nanoparticles at 1.5 Tesla. Diabetes 55: 2931–2938.

32. van Buul GM, Kotek G, Wielopolski PA, Farrell E, Bos PK, et al. (2011) Clinically translatable cell tracking and quantification by MRI in cartilage repair using superparamagnetic iron oxides. PLoS One 6: e17001.
33. Kim JI, Chun C, Kim B, Hong JM, Cho JK, et al. (2012) Thermosensitive/magnetic poly(organophosphazene) hydrogel as a long-term magnetic resonance contrast platform. Biomaterials 33: 218–224.
34. Balakumaran A, Pawelczyk E, Ren J, Sworder B, Chaudhry A, et al. (2010) Superparamagnetic iron oxide nanoparticles labeling of bone marrow stromal (mesenchymal) cells does not affect their "stemness". PLoS One 5: e11462.
35. Nohroudi K, Arnhold S, Berhorn T, Addicks K, Hoehn M, et al. (2010) In vivo MRI stem cell tracking requires balancing of detection limit and cell viability. Cell Transplant. 19: 431–441.
36. Hu SL, Zhang JQ, Hu X, Hu R, Luo HS, et al. (2009) In vitro labeling of human umbilical cord mesenchymal stem cells with superparamagnetic iron oxide nanoparticles. J Cell Biochem 108: 529–535.
37. Kim TH, Kim JK, Shim W, Kim SY, Park TJ, et al. (2010) Tracking of transplanted mesenchymal stem cells labeled with fluorescent magnetic nanoparticle in liver cirrhosis rat model with 3-T MRI. Magn Reson Imaging 28: 1004–1013.
38. Huang DM, Hsiao JK, Chen YC, Chien LY, Yao M, et al. (2009) The promotion of human mesenchymal stem cell proliferation by superparamagnetic iron oxide nanoparticles. Biomaterials 30: 3645–3651.
39. Chien LY, Hsiao JK, Hsu SC, Yao M, Lu CW, et al. (2011) In vivo magnetic resonance imaging of cell tropism, trafficking mechanism, and therapeutic impact of human mesenchymal stem cells in a murine glioma model. Biomaterials 32: 3275–3284.
40. Xiao L, Li J, Brougham DF, Fox EK, Feliu N, et al. (2011) Water-soluble superparamagnetic magnetite nanoparticles with biocompatible coating for enhanced magnetic resonance imaging. ACS Nano 5: 6315–6324.
41. Hart C, Chase LG, Hajivandi M, Agnew B (2011) Metabolic labeling and click chemistry detection of glycoprotein markers of mesenchymal stem cell differentiation. Methods Mol Biol 698: 459–484.
42. Yukawa H, Kagami Y, Watanabe M, Oishi K, Miyamoto Y, et al. (2010) Quantum dots labeling using octa-arginine peptides for imaging of adipose tissue-derived stem cells. Biomaterials 31: 4094–4103.
43. Derossi D, Calvet S, Trembleau A, Brunissen A, Chassaing G, et al. (1996) Cell internalization of the third helix of the antennapedia homeodomain is receptor-independent. J Biol Chem 271: 18188–18193.
44. Noguchi H, Kaneto H, Weir GC, Bonner-Weir S (2003) PDX-1 protein containing its own antennapedia-like protein transduction domain can transduce pancreatic duct and islet cells. Diabetes 52: 1732–1737.
45. Phelan A, Elliott G, O'Hare P (1998) Intercellular delivery of functional p53 by the herpesvirus protein VP22. Nat Biotechnol 16: 440–443.
46. Schwarze SR, Ho A, Vocero-Akbani A, Dowdy SF (1999) In vivo protein transduction: delivery of a biologically active protein into the mouse. Science 285: 1569–1572.

Kuise et al. BioMedical Engineering OnLine 2014, 13:64
http://www.biomedical-engineering-online.com/content/13/1/64

BioMedical Engineering OnLine

RESEARCH Open Access

Establishment of a pancreatic stem cell line from fibroblast-derived induced pluripotent stem cells

Takashi Kuise[1], Hirofumi Noguchi[2*], Hiroshi Tazawa[1], Takashi Kawai[1], Masaya Iwamuro[3], Issei Saitoh[4], Hitomi Usui Kataoka[5], Masami Watanabe[6], Yasufumi Noguchi[7] and Toshiyoshi Fujiwara[1]

* Correspondence: n.hirofumi@cehpnet.com
[2]Department of Surgery, Chiba-East National Hospital, National Hospital Organization, Chiba 260-8712, Japan
Full list of author information is available at the end of the article

Abstract

Background: For cell therapies to treat diabetes, it is important to produce a sufficient number of pancreatic endocrine cells that function similarly to primary islets. Induced pluripotent stem (iPS) cells represent a potentially unlimited source of functional pancreatic endocrine cells. However, the use of iPS cells for laboratory studies and cell-based therapies is hampered by their high tumorigenic potential and limited ability to generate pure populations of differentiated cell types *in vitro*. The purpose of this study was to establish a pancreatic stem cell line from iPS cells derived from mouse fibroblasts.

Methods: Mouse iPS cells were induced to differentiate into insulin-producing cells by a multi-step differentiation protocol, which was conducted as described previously with minor modifications. Selection of the pancreatic stem cell was based on morphology and Pdx1 expression. The pancreatic potential of the pancreatic stem cells was evaluated using a reverse transcription PCR, real-time PCR, immunofluorescence, and a glucose challenge test. To assess potential tumorigenicity of the pancreatic stem cells, the cells were injected into the quadriceps femoris muscle of the left hindlimb of nude mice.

Results: The iPS-derived pancreatic stem cells expressed the transcription factor –Pdx1– a marker of pancreatic development, and continued to divide actively beyond passage 80. Endocrine cells derived from these pancreatic stem cells expressed insulin and pancreatic genes, and they released insulin in response to glucose stimulation. Mice injected with the pancreatic stem cells did not develop tumors, in contrast to mice injected with an equal number of iPS cells.

Conclusion: This strategy provides a new approach for generation of insulin-producing cells that is more efficient and safer than using iPS cells. We believe that this approach will help to develop a patient-specific cell transplantation therapy for diabetes in the near future.

Keywords: Mouse pancreatic stem cells, Diabetes, iPS cells

Background

Production of a sufficient number of insulin-producing cells from stem cells that function similarly to primary islets is important for clinical application of stem cell therapy to diabetes. Many studies have reported the differentiation of insulin-producing cells from mouse embryonic stem (ES) cells and, more recently, from human ES cells [1-7]. Unfortunately, these methods involving ES cells have various limitations such as ethical issues during the generation of the cells and immunological rejection after an

allogeneic transplant. Induced pluripotent stem (iPS) cell technology has the potential to generate patient-specific cell types including functional pancreatic endocrine cells [8-11]. However, the use of ES and iPS cells for laboratory studies and cell-based therapies is hampered by their high tumorigenic potential and limited ability to generate pure populations of differentiated cell types *in vitro*.

D'Amour *et al.* developed a 5-step protocol for differentiation of human ES cells into pancreatic hormone-expressing cells in 2006 [12]; this method represented a great step forward in regenerative medicine; however, the use of ES cells in clinical practice is problematic, as explained above. We and other groups have established mouse pancreatic stem cell lines using specific culture conditions [13-15]. We have also demonstrated that young mice have a high number of pancreatic stem cells that can be isolated, but older mice have a low number of pancreatic stem cells, and therefore are unable to provide viable clones [16]. Similarly, human pancreatic stem cells cannot be isolated from 20- to 60-year-old donors [17].

In this study, we established a pancreatic stem cell line from mouse iPS cells, which have the potential for self-renewal and multipotency to generate both endocrine and exocrine pancreatic cells.

Methods

Culture conditions

Mouse iPS cells (iPS-MEF-Ng-20D-17) were provided by the RIKEN BRC through the Project for Realization of Regenerative Medicine and the National Bio-Resource Project of MEXT, Japan [18]. Undifferentiated iPS cells were maintained on mouse embryo fibroblast feeder layers (STO cell line) in Dulbecco's modified Eagle medium (DMEM; Sigma-Aldrich, St Louis, MO, USA) supplemented with 15% (vol/vol) fetal bovine serum (FBS; Millipore, Billerica, MA, USA), 1% nonessential amino acids (Millipore), 1% nucleosides (Millipore), 1% penicillin/streptomycin (Sigma-Aldrich), 110 μM 2-mercaptoethanol (Life Technologies, Tokyo, Japan), and 500 U/mL leukemia inhibitory factor (LIF; Millipore) at 37°C. Cultures were manually passaged at a 1:4–1:8 split ratio every 3–5 days.

Directed differentiation into insulin-producing cells was conducted as described previously [12], with minor modifications (Figure 1). At stage 1, cells were incubated with 25 ng/mL Wnt3a and 100 ng/mL activin A (R&D Systems, Minneapolis, MN, USA) in the RPMI medium (Life Technologies) at 37°C for 1 day, followed by treatment with 100 ng/mL activin A in RPMI (containing 0.2% FBS) at 37°C for 2 days. At stage 2, the cells were incubated with 50 ng/mL FGF10 (R&D Systems) and 0.25 μM KAAD-cyclopamine (Toronto Research Chemicals, Toronto, Ontario, Canada) in RPMI (containing 2% FBS) at 37°C for 3 days. At stage 3, the cells were incubated with 50 ng/mL fibroblast growth factor 10 (FGF10), 0.25 μM KAAD-cyclopamine, and 2 μM all-*trans* retinoic acid (Sigma-Aldrich) in DMEM with a 1% (vol/vol) B27 supplement (Life Technologies) at 37°C for 3 days. At stage 4, the cells were treated with 1 μM N-[N-(3,5-Difluorophenacetyl)-L-alanyl]-S-phenylglycine t-butyl ester (DAPT; Sigma-Aldrich) and 50 ng/mL exendin-4 (Sigma-Aldrich) in DMEM with a 1% (vol/vol) B27 supplement at 37°C for 3 days. At stage 5, the cells were incubated with 50 ng/mL exendin-4, 50 ng/mL IGF-1 (Sigma), and 50 ng/mL hepatocyte growth factor (HGF; R&D Systems) in the CMRL medium (Life technologies) with a 1% (vol/vol) B27 supplement at 37°C for 3–6 days.

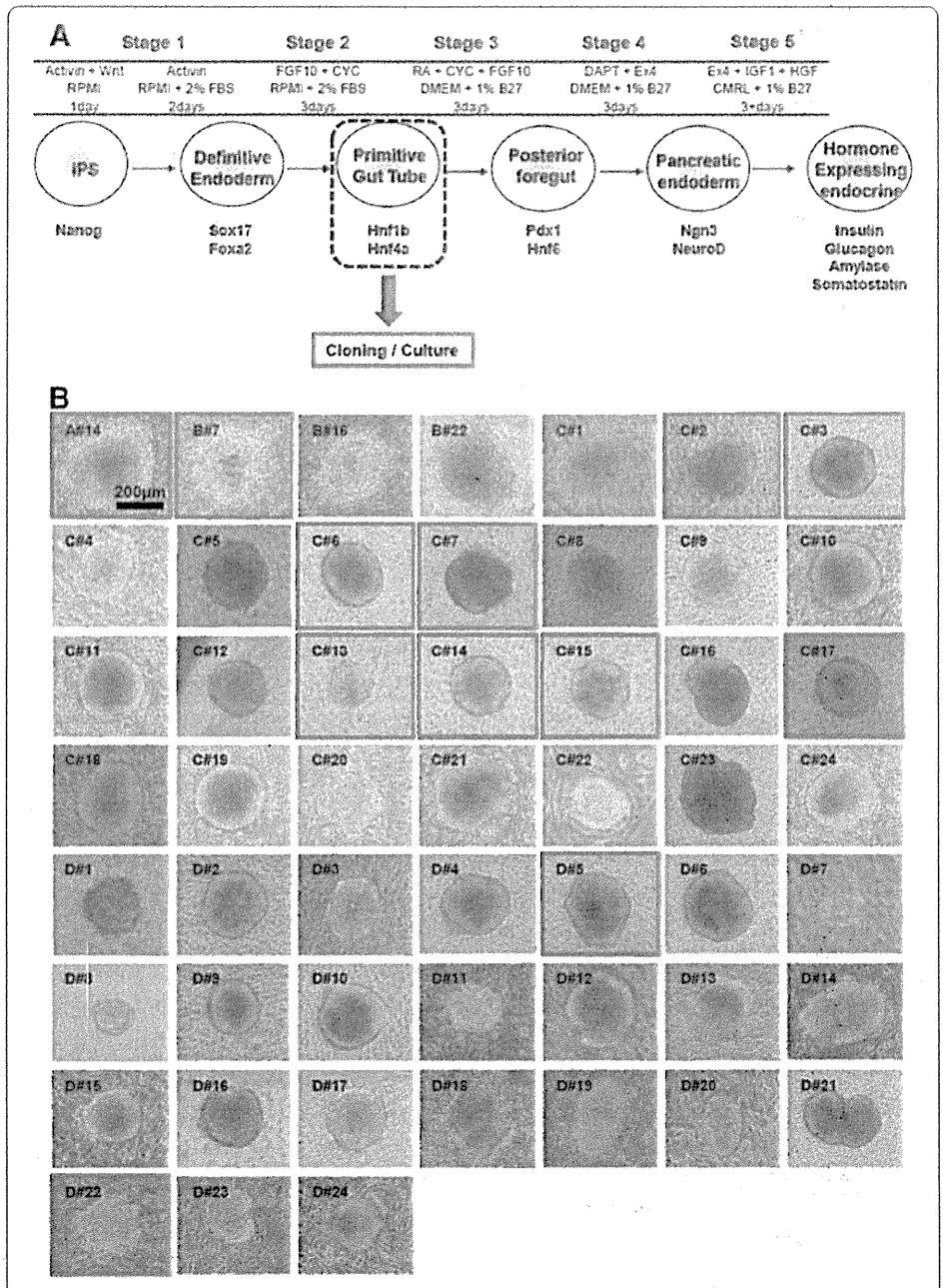

Figure 1 A five-step protocol for differentiation of iPS cells to pancreatic stem cells and hormone-expressing cells. A. Schematic representation of the differentiation procedure and protein expression of key markers of pancreatic differentiation. Based on D'Amour's 5-step protocol [12], this differentiation protocol is subdivided into 5 stages, and the growth factors, medium, and range of duration of each stage are shown. Several markers characteristic of each cell population are listed. Pancreatic stem cells were established after induction of stages 1 and 2. Abbreviations: CYC, KAAD-cyclopamine; RA, all-*trans*-retinoic acid; DAPT, γ-secretase inhibitor; Ex4, exendin-4; iPS, induced pluripotent stem cell; ME, mesendoderm; DE, definitive endoderm; PG, primitive gut tube; PF, posterior foregut endoderm; PE, pancreatic endoderm and endocrine precursor; EN, hormone-expressing endocrine cells. **B**. Morphology of 52 clones after induction of stages 1 and 2 (passage 2). Scale bars = 200 μm.

Tumorigenesis assay

To examine the potential tumorigenicity of candidate clones at passage 50, 1×10^7 cells were injected into the quadriceps femoris muscle of the left hindlimb of nude mice (n = 3). As a positive control, we transplanted 1×10^7 iPS cells into the right hindlimb. All mouse studies were approved by the Institutional Animal Care and Use Committee of Okayama University (Reference number: OKU-2011351).

Semi-quantitative RT-PCR

Total RNA was extracted from cells using the RNeasy Mini Kit (Qiagen, Tokyo, Japan). After the RNA was quantified using spectrophotometry, 2.5 μg of the RNA was heated at 85°C for 3 min and then reverse-transcribed into cDNA in a 25-μL reaction containing 200 units of Superscript III RT (Life Technologies), 50 ng of random hexamer primers (Life Technologies), 160 μmol/L dNTP, and 10 nmol/L dithiothreitol. The reaction consisted of 10 min at 25°C, 60 min at 42°C, and 10 min at 95°C. PCRs were performed in a Perkin-Elmer 9700 Thermocycler with 3 μL of cDNA (20 ng RNA equivalent), 160 μmol/L cold dNTPs, 10 pmol of the appropriate oligonucleotide primers, 1.5 mmol/L $MgCl_2$, and 5 units of AmpliTaq Gold DNA polymerase (Perkin-Elmer, Waltham, MA, USA). The oligonucleotide primers and cycle numbers used for semi-quantitative PCR are shown in Table 1. The thermal cycle profile used a 10-min denaturing step at 94 C followed by the amplification cycles (1 min denaturation at 94 C, 1 min annealing at 57 C, and 1 min extension at 72°C), with a final extension step of 10 min at 72°C. The steps taken to validate these measurements were previously reported [19].

TaqMan real-time PCR

Quantification of Ngn3, NeuroD, and insulin-2 mRNA levels was conducted using the TaqMan real-time PCR system according to the manufacturer's instructions (Life Technologies). PCR consisted of 40 cycles including 2 min at 50°C and 10 min at 95°C as initial steps. In each cycle, denaturation was performed for 15 s at 95°C and annealing/extension was 1 min at 60°C. PCR was conducted in 20-μL reaction containing cDNA synthesized from 1,500 ng of total RNA. Standard curves were constructed using cDNA generated from total RNA isolated from primary mouse islets. For each sample, the expression of Ngn3, NeuroD, and insulin-2 was normalized against the β-actin expression level. Mouse Ngn3, NeuroD, and insulin-2 and β-actin primers were obtained commercially (Assays-on-Demand Gene Expression Products; Life Technologies).

Table 1 List of gene-specific primers

Gene	Forward/Reverse primer (5′ → 3′)
Nanog	cacaggctctttcttcagattg/tcttgcttgctcttcacattgg
Pdx1	cggacatctccccatacg/aaagggagctggacgcgg
Insulin-2	tccgctacaatcaaaaaccat/gctgggtagtggtgggtcta
Glucagon	agaagggcagagcttgggcc/tgctgcctggccctccaagt
Amylase	tggccttctggatcttgc/aaaggtctgcttccttggg
Somatostatin	atgctgtcctgccgtctc/ttctctgtctggttgggctc
Gapdh	accacagtccatgccatcac/tccaccaccctgttgctgta